Detection of Earth-like Planets with NWO

With discoveries like methane on Mars (Mumma et al. 2009) and super-Earth planets orbiting nearby stars (Howard et al. 2009), the fields of exobiology and exoplanetary science are breaking new ground on almost a weekly basis. These two fields will one day merge, with the high goal of discovering Earth-like planets orbiting nearby stars and the subsequent search for signs of life on those planets. The Kepler mission will soon place clear bounds on the frequency of terrestrial-sized planets (Basri et al. 2008). Beyond that, the great challenge is to determine their true natures. Are terrestrial exoplanets anything like Earth, with life forms able to thrive even on the surface? What is the range of conditions under which Earth-like and other habitable worlds can arise? Every stellar system in the solar neighborhood is entirely unique, and it is almost certain that anything that can happen, will.

With current and near-term technology, we can make great strides in finding and characterizing planets in the habitable zones of nearby stars. Given reasonable mission specifications for the New Worlds Observer, the layout of the stars in the solar neighborhood, and their variable characteristics (especially exozodiacal dust) a direct imaging mission can detect and characterize dozens of Earths. Not only does direct imaging achieve detection of planets in a single visit, but photometry, spectroscopy, polarimetry and time-variability in those signals place strong constraints on how those planets compare to our own, including plausible ranges in planet mass and atmospheric and internal structure.

Such a mission also would precipitate revelations about the entire architectures of nearby star systems and, given the right mission design, could easily accommodate a wide array of revolutionary astrophysical and cosmological programs. **A mission dedicated to the direct imaging and characterization of habitable planets is an achievable goal which would not only garner wide approval from the general public but would yield significant advances in astrophysics as a whole.**

Our key findings are as follows:

1. Direct imaging at an inner working angle of 50 milliarcseconds with a limiting planet:star contrast ratio of a few times 10^{-11} allows significant probability (>20%) of single-visit detection and characterization of Earth-like planets in the habitable zones of at least 93 stars, with a net of 35.8 total habitable zones searched, within a mission lifetime of a few years. Those stars are primarily F- (4), G- (59), and K- (28) type dwarfs. This is a conservative estimate, however, and does not account for e.g., the ability to detect fainter planets at angles larger than the IWA.

2. Efficient planet detection/characterization is possible even with high levels of exo-zodiacal light (10 times solar levels or more). A pre-cursor mission (e.g., astrometry) is not required for efficient planet detection and characterization via direct imaging. Unresolved background objects are likely to occur but can be efficiently ruled out by color photometry and spectroscopy.

3. To prepare for any mission to find habitable exoplanets, it is crucial to expand “nearby stars” observing campaigns to identify faint companions (both physical companions and distant background objects), exozodiacal dust levels, and stellar characteristics such as variability (especially useful for transit searches), metallicity, and age estimates. Such observations would

greatly aid in (1) target selection and (2) our interpretation of the data to understand where habitable planets can form and how they evolve over time.

The Target Stars

Because a star's habitable zone is located so near to the star itself, the technology for any mission to image habitable worlds is driven toward extremely high contrast imaging at very small star-planet angular separations. In this paper we are guided by a specific mission concept into which we have invested detailed consideration as part of an Astrophysics Strategic Mission Concept Study, i.e., NASA's New Worlds Observer (NWO). This 4-m telescope plus starshade concept provides for a planet:star limiting contrast of a few times 10^{-11} or deeper at an inner working angle of ~50 milliarcseconds.

Given those specifications, the most important question in assessing the viability of a direct imaging planet-finding mission is: Given the layout of stars in our neighborhood, which star systems can be searched for Earths? The answer (expressed both in number of stars and types of systems) determines whether any such mission is scientifically viable.

Habitable Zone Size

The true location of the habitable zone around a star (where the temperature allows for liquid water on the planet's surface) depends on the atmospheric and geological processes at work in the planet under consideration (e.g., Kasting, Whittet & Sheldon 1996). We can simplify the discussion by noting that for an Earth-like planet, the inner HZ edge does not extend as close to the Sun as 0.7 AU (i.e., Venus). The outer edge is less well-constrained but apparently extends to at least 1.5 AU, because Mars appears to have had copious amounts of surface water in the past, and a more massive planet (with higher surface gravity and carbon cycling) may have remained habitable to this day. The HZ limits for the Sun used here are from 0.7 to 1.5 AU. These limits define the amount of energy a planet can receive to be inside the habitable zone, and to calculate the inner HZ (IHZ) and outer HZ (OHZ) limits for other stars, we scale by the square root of stellar luminosity:

Inner HZ = a_{IHZ} = 0.7 AU $\times \sqrt{L_* / L_{sun}}$
Outer HZ = a_{OHZ} =1.5 AU $\times \sqrt{L_* / L_{sun}}$

In this paper, stellar luminosity is calculated using V-band bolometric corrections from Flower (1996) and Hipparcos corrected Johnson B-V values (Bessel 2000; Turnbull 2004). Translating the linear HZ size in AU into an angular size, we find that the angular HZ size can be expressed in terms of the apparent magnitude alone:

$$\vartheta_{HZ}('') = a_{HZ}(AU)/d(pc) = \sqrt{(L_* / L_{sun})} \Big/ d(pc)$$
$$= \sqrt{10^{-(M_{BOL}-4.8)/5}} \,/ d(pc).$$

Taking $M_{BOL} \approx M_V$ and $M_V = V - 5 \log d(pc) - 5$, a convenient rule of thumb is:

$$\theta_{HZ}('') \approx 10^{-V/5}.$$

Thus for a habitable-planet-finding observatory with a ~50 milliarcesecond inner working angle (IWA, the smallest angle where planets can be detected above the stellar signal), no target shall be fainter than V~6.5. **This means that from our place within the Solar Neighborhood, the latest spectral type searchable with an inner working angle of 50 mas is ~K5V.** Late K and M stars, it would seem, are indeed better suited for transit studies (Gould, Pepper & DePoy 2003). Additionally, sunlike stars beyond a distance of 20 pc are not available to such a design.

Hipparcos' limiting magnitude is V~12, but the catalogue is *complete* only down to V=7.3-9 (depending on star color). As a result, the 30 pc sample of stars is complete for G-, F-, A-, and B-type stars and giants, but not for the fainter K- and M-stars. However, as seen above, these faintest stars are of less interest to us in direct imaging: despite the favorable contrast ratio (discussed below), their habitable zones are too small to resolve and their planets are too faint to characterize. Therefore the sample of 2100 Hipparcos stars within 30 pc includes every viable direct-detection target star, and many more.

Planet-Star Contrast Ratio

In addition to being very near to the star, a habitable terrestrial planet is very small in size, and thus reflects only a tiny fraction of the star's light. The amount of starlight reflected by a planet in the habitable zone depends on three things: its distance from the star within the HZ, the planet's radius, and the planet's albedo at the wavelength of the detection bandpass. Planet luminosity does *not* depend on the luminosity of the star; by definition, "the habitable zone" is where the planet receives the right amount of energy for an Earthlike planet to have liquid water on its surface (about 10^{24} ergs sec^{-1} cm^{-2}), regardless of which star it orbits. (That said, the planet's location *within* the habitable zone does affect the planet's brightness; planets at the outer edge of the HZ are fainter than at the inner edge, by a factor of ~4.6.)

A useful note, then, is that for planets of a given size and albedo, the planet-star contrast depends only on the stellar luminosity: $\left(F_p / F_*\right)_{HZ} = 1.155 \times 10^{-10} / L_*$ at the Earth-equivalent insolation distance (which is 1 AU for the Sun). This brings home the challenge for planet-imaging missions: that angular habitable size goes as the stellar luminosity L_*, while fractional planet brightness goes as $1/L_*$, and both are quantities that we wish to maximize.

The Earth is near the inner edge of its habitable zone and is thus brighter than the average habitable planet might be. For a limiting contrast ratio of 10^{-10} (a number often used as the baseline requirement for direct imaging), a sun-like star is too luminous for detection of an Earth at the outer HZ. Indeed, a 10^{-10} contrast requirement would mean that the maximum luminosity for stars whose planets are detectable at the outer HZ is only ~0.5 L_{sun}. Requiring that the entire HZ be searchable would thus rule out stars brighter than spectral type ~G8V from the target list. At the inner HZ, this maximum luminosity is 2.4 L_{sun}, or ~F5V. It is for this same reason (i.e. contrast) that A- and early F-type stars and giants could be difficult targets in the visible band.

However, there need not be a sharp cutoff in planet detectability when the planet-star separation is equal to the IWA or when the planet-star contrast is equal to starlight suppression level. For a starshade design like NWO, planets should be detectable at several times below the starlight suppression level, given sufficient integration time. A limiting contrast "floor" (below which, due to systematic effects, no amount of integration time results in a detection) of a few times 10^{-}

^{11} is feasible for such a system. Suppression of starlight also improves at larger working angles, meaning that fainter planets at wider angular separations (i.e., for nearby systems) can still be detected. A starshade mission also does not have an outer working angle (Cash 2006) and this means that the nearest star system, alpha Centauri, would be a viable target in the search for Earths.

Completeness

To assess the number of target stars available for a given mission and to provide a means of judging the relative science return from each star, we calculate the *completeness* for each star on the 30 parsec Hipparcos list. For each star, we create a set of orbits within the HZ and populate them with planets. We then make cuts at the IWA and contrast limit and determine what fraction of the planets would have been detected. This fraction is the completeness for that star, which can also be thought of as the probability of finding a HZ resident at that star, if every star has 1 such planet (i.e. η_{Earth}=1). For simplicity at this time, we assume that planets are visible if they are farther from their parent star than the IWA and have a fractional brightness greater than the contrast floor. We also assumed Earth-twin planets with a constant size and albedo. In the future, we can take into account the variation of planet detectability with offset and contrast as well as a range of planet characteristics.

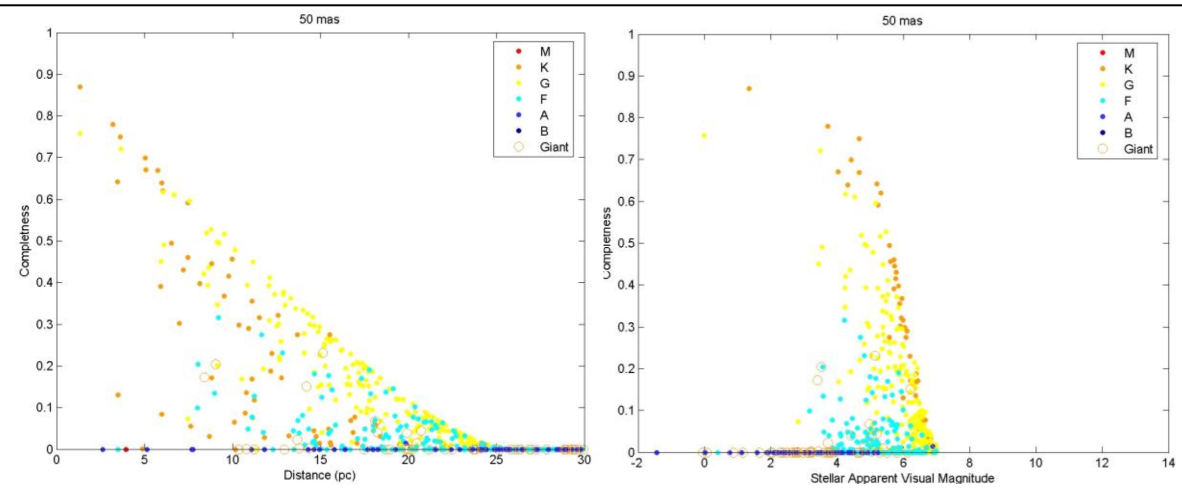

Figure 1: *Completeness vs. distance (left) and completeness vs. brightness (right) for Hipparcos stars within 30 parsecs, color-coded according to spectral type.*

Figure 1 shows completeness for the stars within 30 pc, as a function of distance and apparent magnitude. Completeness quickly falls to near zero for stars fainter than V~6.5. The nearest K stars top the list in terms of likelihood of detecting an Earth in the habitable zone, followed by G dwarfs (which have smaller planet:star contrast but larger angular HZs) out to ~20 pc. For IWA of 50 mas and contrast floor of $4x10^{-11}$, there are 93 stars with a completeness of greater than 20%, for a total of 35.8 habitable zones searched.

This represents a conservative estimate, as we have not taken into account effects such as the ability to detect planets fainter than this at larger working angles (note that there is no outer working angle for a starshade). For example, alpha Centauri A, a sun at 1pc, has an angular habitable zone that is entirely visible outside the IWA, extending from ~70 mas to 1500 mas. Our calculations put the system at only ~75% completeness, however, due to the higher contrast ratio required to see Earths orbiting early G-type stars. In reality, this star likely has nearly 100% completeness because a deeper contrast ratio can be achieved at these larger working angles. Meanwhile, the innermost habitable zone of alpha Cen B is just inside the 50 mas IWA, giving ~87% completeness, but planets in that system would be fractionally brighter and may still be detectable.

Distinguishing Planets and Their Orbits

In order to find and characterize exoplanets using direct detection, we not only need to see the planet's light, we also need to distinguish between planets and background sources, differentiate between multiple planets in a extra-solar system, and measure the orbits of planets we find.

Exo-zodiacal Light and Mission Lifetime

An important question in direct imaging of habitable planets is whether dust in the system will overwhelm the planet signal. Figure 2 shows, for Hipparcos stars within 30 parsecs, the integration times required to detect Earth-like planets at quadrature (M_V = 30) at S/N=10, assuming every star has an exozodiacal light level of 10 times the solar value. Choosing targets to maximize completeness and limit total integration time to 1 year (for both detection and spectroscopy) results in a favored sample of primarily G- and K-type stars (shown in color). For a starshade mission, the total mission lifetime would also include transit of the starshade between targets. Our mission planning simulations show that 30-50% of the total observing time would be spent on these exoplanet science targets, with the remaining 50-70% available to general astrophysics while the starshade is in transit to the next exoplanet target.

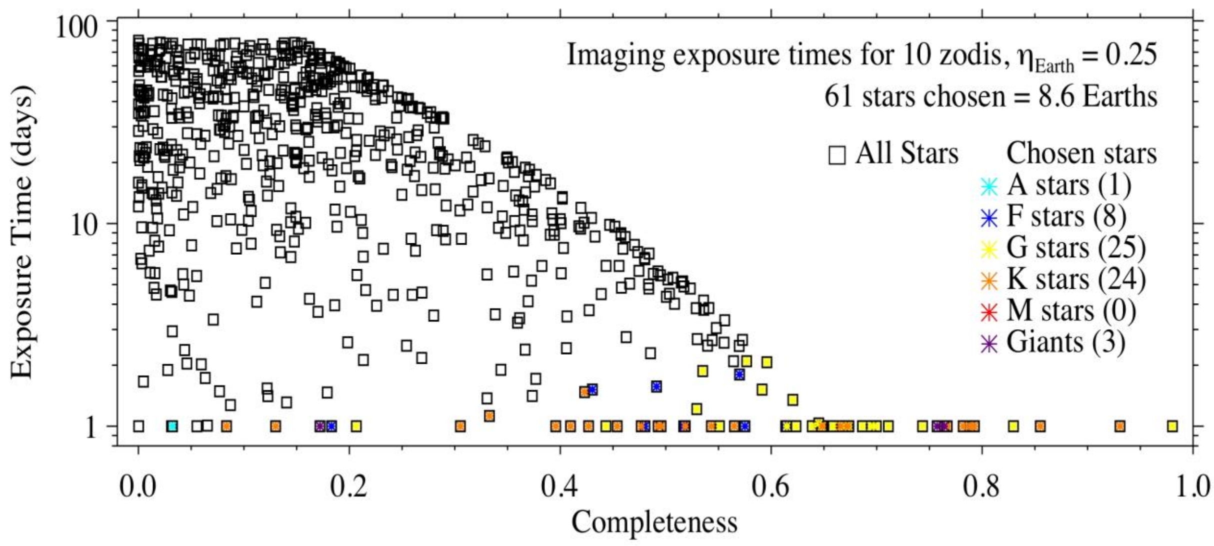

Figure 2: *Colored asterisks corresponding to different types of stars show the targets in a possible observing program lasting 1 year (including imaging and spectroscopy), assuming $\eta_{Hab.\ Earth}$ = 0.25. For each type of star, the number chosen for observation appears in parentheses to the right of the type label. Most selected stars are G and K type; no M stars were chosen. In this scenario, 61 stars are observed, giving 34.4 total HZs searched and 8.6 Earths characterized. Instrumental assumptions used here are consistent with a starshade mission: observatory throughput = 50%, telescope diameter = 4-m.*

Background Objects

Depending on galactic latitude and longitude, background sources will unavoidably appear in many of our target fields. In order to identify a point source in the field as a planet, we need to be able to differentiate between planets and background stars or distant galaxies. The stellar background at magnitudes below V~28 is not well characterized but can vary wildy depending on galactic latitude and longitude. Near the galactic poles, the odds for a background galaxy contamination can be as high as several hundred sources per square arcminute (Beckwith et al. 2006), or several tens of sources in the field of interest around a target star. Most bright galaxies will be resolved, but faint unresolved galaxies (near V~30) are potential sources for confusion that can be ruled out (or determined to be unlikely planet candidates) through a combination of color photometry and proper motion.

Because planets are seen in reflected starlight, even low resolution spectra (and in many cases broadband photometry) can immediately distinguish whether these objects are indeed associated with the star in question. Furthermore, given that the viable target stars are all within ~20 pc of the Sun, they have relatively high proper motions. Therefore it will not take much time at all for a potential planet to be confirmed as co-moving with the target star. In fact, common proper motion objects can usually be confirmed within a single observing session of a few weeks. Bright exo-zodiacal clumps, interesting in their own right, may require spectra to distinguish them as non-planets.

Multiple Planets

If multiple planets are seen in an initial observation of a stellar system, there is a worry that it might be unclear which planets are which when we return to the system for a second observation. In fact, it is relatively easy to determine the identity of each planet just based on its position in the field at the two times. In addition, if colors and even spectra are taken of each planet immediately after it is discovered, a unique identity can be established.

Orbit Determination

Another perceived difficultly of using direct-detection to search for exoplanets is that it would be difficult to determine the orbit of any planets that are found. In fact, direct images of a stellar system have several advantages. The two-dimensional position of each planet is determined in each observation, which gives more information per observation than e.g. radial velocity or astrometry measurements. Any dust that is present in the system (proto-planetary, debris, or exo-zodi) will most likely be arranged in a disk with a discernable inclination. We expect planets in the system to have orbits with a similar inclination to this disk, which eliminates a source of degeneracy.

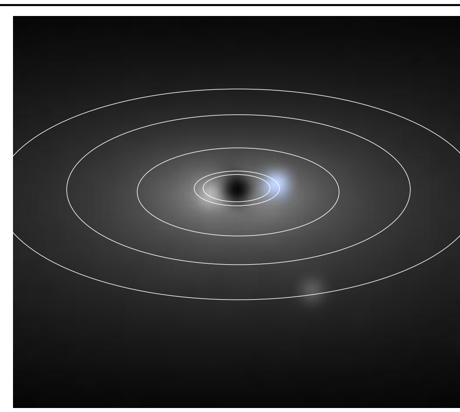

Figure 4: If exozodiacal light can determine inclination and orientation of ecliptic plane, then, under assumption of circularity, orbits of planets may be immediately determined.

Requirements (and Non-requirements) for Direct-Detection Missions

To summarize, the basic requirements for a successful search for terrestrial exoplanets with a direct-detection mission are limiting planet:star contrast ratio of a few times 10^{-11} and an IWA < ~50 mas. The success of the mission will be improved by the ability to immediately get several colors of the planets (to distinguish planets from background sources). Good photometric accuracy is also important in order to detect longer term variability in planet signals due to phases, rotation, and seasons. The ability to take a spectrum of each planet shortly after its discovery will allow an assessment of atmospheric composition, surface signatures, habitability and possibly biosignatures. Imaging the entire solar system at once is critical in order to study outer planets, debris disks, and exozodiacal structure. In order to determine the orbit of the detected planets, the mission must be able to revisit the system 2-3 times.

It is useful to note here that a pre-determined list of exo-planet targets is NOT a requirement for a successful direct-detection mission. Since planet detection and characterization takes less than several days (for starshade missions), all of the viable targets can be studied within a mission lifetime of ~5 years. Indirect-detection precursor missions (e.g., astrometry missions) add little to the efficiency of a direct imaging program and are perhaps most useful as follow-up programs for precise mass and orbit determinations.

References

Basri, G., Ramos-Stierle, F., Soto, K., Lewis, T., Reiners, A., Borucki, W., Koch, D. 2008, "The Kepler Mission: Terrestrial Extrasolar Planets and Stellar Activity", 14th Cambridge Workshop on Cool Stars, Stellar Systems, and the Sun ASP Conference Series, Vol. 384, Ed. Gerard van Belle., p.281

Beckwith, S. et al. 2006, "The Hubble Ultra Deep Field", AJ, 132, 1729

Bessell, M. S. 2000, PASP, 112, 961

Cash, W., 2006. "Detection of Earth-like planets around other stars using petal-shaped occulters", *Nature*, 442, 51-53

Flower, P. J. 1996, ApJ, 469, 355

Gould, A., Pepper, F. & DePoy, D. L. 2003, ApJ, 594, 533

Howard, A. W., Johnson, J. A., Marcy, G. W., Fischer, D. A., Wright, J. t., Henry, G. W., Giguere, M. J., Isaacson, H., Valenti, J. A., Anderson, J., & Piskunov, N. E., 2009, "The NASA-UC Eta-Earth Program: I. A Super-Earth Orbiting HD 7924), accepted to ApJ

Kasting, J. F., Whittet, D. C. B., & Sheldon, W. R. 1996, OLEB, 27, 413

Mumma, M. J., Geronimo L. Villaneuva, Robert E. Novak, Tilak Hewagama, Boncho P. Bonev, Michael A. DiSanti, Avi M. Mandell, and Michael D. Smith. 2009, "Strong Release of Methane on Mars in Northern Summer 2003", Science Express, 15 January 2009

Turnbull, M.C. 2004, PhD Thesis, University of Arizona

Planetary Characterization

In order to characterize the physical properties of an extra-solar planet one needs to detect planetary radiation, either visible (VIS) to near-infrared (NIR) reflected starlight or infrared (IR) thermal radiation. Both the reflected and thermal flux depend on the size of the planet, the distance between the planet and the star, the distance between the observer and the planet, and the planet's phase angle (i.e. the angle between the star and the observer as seen from the planet). Moreover, the planetary radiation also depends on the composition and structure of the planet's atmosphere and/ or surface, the wavelength of the observation, and other effects such as the presence and physical characteristics of planetary rings or moons. This section describes the techniques needed to learn about the properties of the planet from various observations of its radiation. Previously we discussed how planets might be found using direct-detection methods; here we focus on the more detailed photometry, spectroscopy, polarimetry, and time-variability that can reveal the true nature of these planets and the systems in which they were born.

Recently, transit techniques have been extremely successful in providing the first information about the atmospheric composition and structure of a selected number of Giant and Neptune-size planets orbiting very close to their parent stars. With the launch of JWST, these methods will have the ability to study large, hot, rocky planets, but they will still be unable to characterize Earth-like planets within the "habitable zone" of F, G, and K stars. Direct imaging of rocky Earth-size planets in the habitable zone requires subarcsecond angular resolution at contrast ratios of a few times 10^{-11} in order to remove the bulk of the signal originating from the central star.

Such observations are not currently possible, but can become so in the coming decade with a properly configured space mission. Coronagraphic techniques now exist that can efficiently separate the exoplanet light from the glare of the parent star. We discuss some of the key observations that can be made if the observatory provides the same capabilities for exoplanet studies that are routinely made now on faint stars. The authors believe that all of the observations described herein would be possible in the coming decade using an external occulter system such as the New Worlds Observer, which has just completed an Astrophysics Strategic Mission Concept Study.

Planetary albedo and mass

The reflected planetary radiation depends on clouds, aerosols, and surface types, all of which can highly influence the planetary reflectivity (albedo). Signatures of this influence will be detectable in broad-band photometric observations (Fig. 1). The planet's albedo will be derived from the reflected flux by assuming a planet radius. For massive (down to Saturn-mass) planets, all models agree that the radius is very close to one Jupiter radius. For lighter planets, we can make use, to first order, of mass-radius

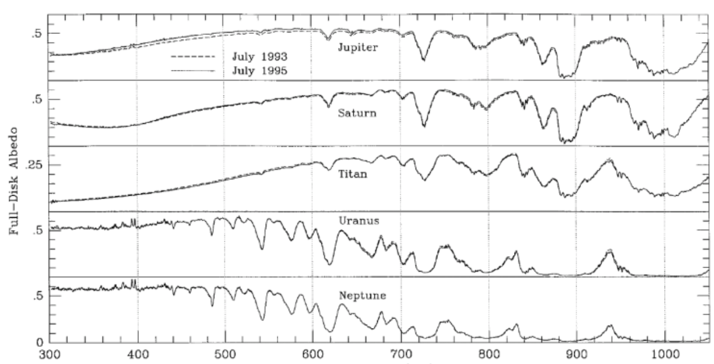

Figure 1: *Observed albedo for the gas giant planets and Titan in our Solar System (Karkoschka 1998)*

relations (Sotin et al. 2007; Valencia, O'Connell, & Sasselov 2006; Fortney et al. 2007). If a planet has been detected with radial velocity or astrometry measurements, its mass can be derived when combined with the observed orbital inclination angle. Depending on a planet's composition, its radius can vary by a factor of up to 20% for a given mass which translates into an uncertainty of 40% in the albedo. The value of the albedo can be further refined using flux and polarization spectra, time variability, and theoretical models as discussed below.

For all these reasons we argue that, while measuring the mass of the planet astrometrically is an important parameter for detailed modeling, the most important information is gained through direct observation. Measurement of mass should follow planet detection and classification, as opposed to being a necessary first step.

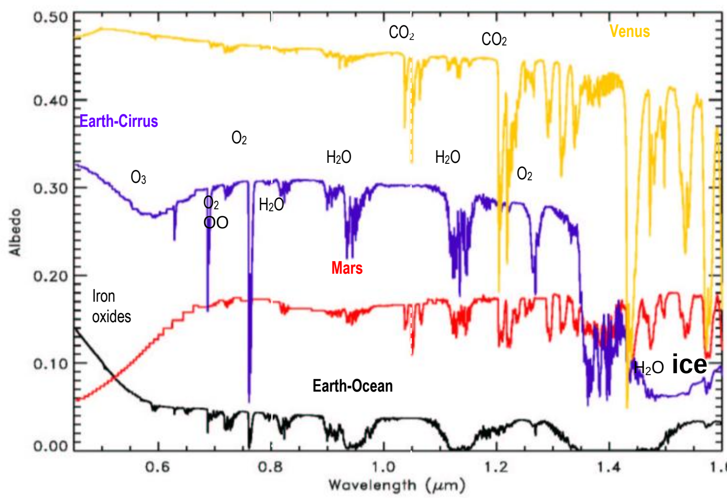

Fig. 2: *Albedo simulations of cloudy and cloud-free Earth (violet and black), Venus (yellow), and Mars (red).*

Spectroscopy and atmospheric species

Spectroscopy of the planetary radiation will provide very rich information, such as the species present in the atmosphere and the cloud coverage (Fig. 2). Table 1 lists the atmospheric gas molecules with absorption bands in the VIS/NIR bands.

Water is the necessary ingredient for the types of life found on Earth and it has played an intimate, if not fully understood, role in the origin and development of life on Earth. Water also contributes to the dynamic properties of terrestrial planets, permitting convection within the planetary crust that might be essential to supporting Earth-like life by creating local chemical disequilibria that provide energy. There are absorption bands from water though much of the VIS/NIR spectrum with a very distinctive spectral signature.

In addition to water, the search for carbon-dioxide is of special interest. Its presence would indicate (1) that carbon is available for the biosphere, (2) a (natural) greenhouse effect, and (3) a possible regulation by the hydro- and geosphere.

The greatest surprise in the composition of the planets in our solar system is the large amount of oxygen in the terrestrial atmosphere. This molecule is so reactive chemically that it must be continuously produced at enormous rates to persist. Thus the Earth's atmosphere can only be the result of a large input from the biosphere (Lovelock 1979). The challenge of remotely detecting life on a planet that has not developed a biogenic source of oxygen is fraught with unknowns. O_2 has its strongest spectral signature in the visible wavelength range.

Molecule	Absorption bands (μm)
H_2O	0.51, 0.57, 0.61, 0.65, 0.72, 0.82, 0.94, 1.13, 1.41
CH_4	0.48, 0.54, 0.57. 0.6, 0.67, 0.7, 0.79, 0.84, 0.86, 0.73, 0.89, 1.69
CO_2	1.21, 1.57, 1.6.
NH_3	0.55, 0.65, 0.93, 1.5
O_3	0.45-0.75 (the Chappuis band)
O_2	0.58, 0.69, 0.76, 1.27
CO	1.2, 1.7, 2.4

Table 1: *Absorption bands of the most important atmospheric molecules that can be detected and identified in the visible/near-infrared.*

Water, oxygen, methane, carbon dioxide and ammonia give the key signatures for characterizing atmospheres of exoplanets.

Time variability

Direct imaging of exoplanets may also reveal time-variability in the planet's flux and/or spectra. This variability could arise from daily rotation (with different parts of the planet rotating into view), from the orbital movement of the planet (which will generally change the phase angle), or from delayed impact of stellar activity. There might also be time-dependent changes on the planet itself due to weather and seasons.

A key indicator of the presence of liquid surface water is higher than expected reflectivity and variability at crescent phases when the system is observed at high inclination. This is due to the intensity of specular reflection off of the (somewhat) smooth ocean surface: the reflected light is concentrated at a reflected angle equal to the incident angle, much like a mirror (Williams & Gaidos 2008). Figure 3 shows that the behavior of the light curve at crescent phases may tell us if the planet has water-like features on the surface. The intensity of specular reflection causes the average daily brightness to be somewhat greater than for a land-only planet. Additionally, as clouds or land features temporarily obscure this specular reflection, the planet will significantly dim, causing potentially higher hourly variability (Oakley & Cash 2009).

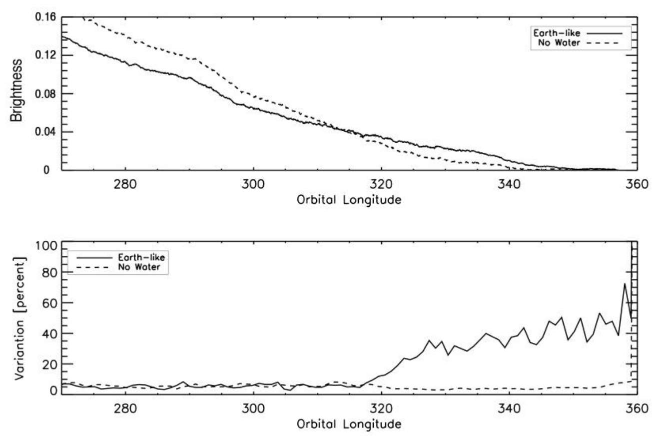

Fig. 3: *The detection of liquid surface water may be possible through studying the planet's photometric behavior at crescent phases. The top plot shows the average daily brightness of the planet, while the bottom planet shows the shorter-term variability that has been smoothed out in the top plot.*

These observations will be crucial in discovering oceans, however the crescent phase is the most difficult time to observe a planet, due to decreased signal strength, increased noise (due to stronger exo-zodiacal signal), and observational effects due to the planet approaching the inner working angle of the system. This should stress the importance of having an observing system with the smallest possible inner working angle.

It is also possible to measure diurnal flux changes for an Earth-like planet from long-term photometric monitoring (Ford et al. 2001; Tinetti et al. 2006; Hearty et al. 2008; Palle et al. 2008; Oakley et al. 2008). These effects were simulated and it was shown that, given several days of observation time, the periodic tendencies of the light curve can lead to an accurate determination of the rotation rate of the planet (Figure 4). A Fourier power analysis or an autocorrelation analysis typically indicates a 24-hour rotation rate for >50% of attempts with a broadband signal-to-noise range of 5-10 and has near perfect success for most geometries given a SNR of 20 or higher (Palle et al. 2008; Oakley et al. 2008). The analysis at lower SNR often returns a 12-hour rotation rate, which is not surprising given that the Earth consists of two main landforms interspersed by two main oceans. The changing cloud cover is the dominant source of confusion rather than noise introduced by external factors such as exozodiacal light.

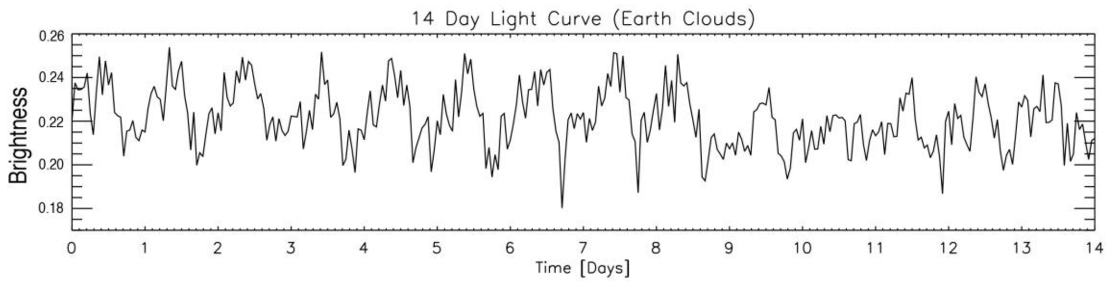

Fig. 4: *Sample data over 14 days of observation. The hourly variation is due to the changing disk-averaged albedo of the planet as clouds and surface features rotate into view. Given sufficient observation time, the rotation rate of the planet can be accurately determined.*

Time variability in spectra can also provide information about the distribution of surface types, aerosol, and clouds. For example, flux and polarization spectra of cloudy planets are expected to be very sensitive to phase, both in the total amount of light and in the shape of the spectra (the continuum shape and the absorption band depths) due to related changes in atmospheric path-length above the clouds and the changing position of the observer with respect to the star).

Polarimetry

With polarimetry, one measures the flux at a given polarization angle and determines the degree of polarization of the light (the fraction of polarized flux to the total flux). Polarimetry can help to distinguish (polarized) planetary light against the background of (unpolarized) direct starlight. It can help to quickly confirm that the dot of light that is detected in the vicinity of a star is indeed a planet and not e.g. a background star. Polarimetry can also be used to characterize the planet because the degree of polarization of the light scattered from a planet varies with the planetary phase angle and also depends strongly on the properties of the planetary atmosphere and/ or surface.

Starlight is virtually unpolarized, while the light that has been reflected by a planet orbiting the star will usually be polarized because it has been scattered within the planetary atmosphere or reflected by the planetary surface. The degree of polarization observed depends on the degree of polarization of the planet itself and on the background of residual, unpolarized starlight: the smaller the background flux, the closer the observed degree of polarization will be to the planet's degree of polarization. For exoplanets that can be spatially resolved from their star, the observable degree of polarization can reach several tens of percents in the extreme case of no background starlight (Stam et al. 2004).

Because the planet's light is significantly more polarized that the star's light, polarimetry observations can help to pull the signal of the planet from the background of unpolarized starlight. In addition, if the potential exoplanet is found to have a significant level of polarization, this can immediately confirm its nature as a planet rather than a background star. Such an instant confirmation eliminates having to wait to check whether the detected dot is actually in orbit around the star. There is even a relation between the direction of polarization and the imaginary line connecting the planet and its star: the direction of polarization of the reflected starlight will always be parallel or perpendicular to this line except for planets with strong horizontal inhomogeneities or very bright rings. This can help narrow down the possible orbits of the exoplanet in a single observation.

The degree of polarization of an exoplanet usually varies strongly with planetary phase angle because the scattering processes within the atmosphere depend strongly on the planet's illumination and viewing geometries (Fig. 5). In particular, the degree of polarization of an exoplanet will usually be highest for intermediate phase angles, when the angular separation between the planet and the star is largest and the planet should be easiest to detect. For phase angles near 0 and 180 degrees, the planet's degree of polarization will always be close to zero; however even a planet in a wide orbit cannot be spatially resolved from its star at these phases and is thus not observable with a direct-imaging technique.

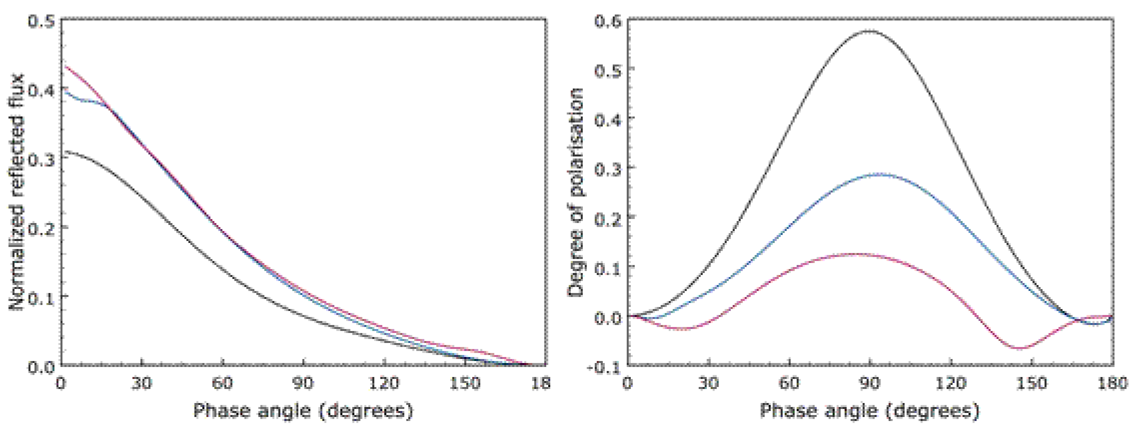

Fig. 5: *The flux (left) and degree of polarization (right) of starlight that is reflected by three model gaseous planets as functions of the planetary phase angle. The black line is a Jupiter-like planet with a pure molecular atmosphere, blue is the same planet except with an optically thick cloud layer in the troposphere, and purple is a cloudy planet with a thin stratospheric haze, each averaged over λ= 0.65 to 0.95 microns (Stam et al. 2004).*

Furthermore, polarimetry can be used to characterize the planet since the degree of polarization of a planet and its variation with phase angle depend strongly on the properties of the planet. Since the planet's reflection properties usually depend on the wavelength, the degree and direction of polarization also usually depend on the wavelength (Fig. 6). Indeed, the optical properties of the planetary atmosphere and surface have a larger influence on the degree of polarization of reflected starlight than on the flux (Hansen & Hovenier 1974).

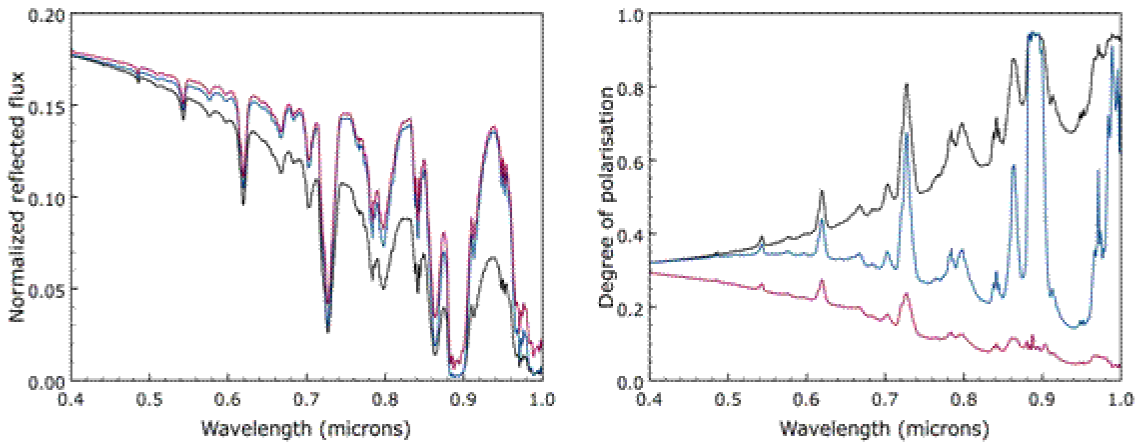

Fig. 6: *The flux (left) and degree of polarization (right) of starlight that is reflected by the three model gaseous planets described in Fig. 4 for planetary phase angles of 90 degrees. The fluxes have been normalized such that at a phase angle of 0 degrees, they equal the planet's geometric albedo (Stam et al. 2004).*

If the planet is embedded in a circumstellar disk, the dust particles in the disk will also scatter polarized starlight. However, because the microphysical properties of these particles will differ strongly from those in the planetary atmosphere, their polarization signatures will differ from that of the planet. Especially when the planet's polarization signature is measured across a range of wavelengths and at different planetary phase angles, we will be able to make a clear distinction between the planet and its environment. The polarimetry can also be used to characterize the circumstellar dust particles themselves.

The degree of polarization is a relative measure (the polarized flux divided by the total flux). As such, it is independent of the size of the planet and its distance to the star. Being able to characterize a planet without having precise information on these parameters is a strong advantage of polarimetry. Especially by combining flux with polarization measurements, planet characteristics can be retrieved that would be inaccessible by flux measurements alone. For example, the reflected flux is not sensitive to cloud-top altitudes, while the degree of polarization is. The flux, however, is sensitive to the optical thickness of the cloud, while the degree of polarization is less sensitive to this.

Thanks to the obvious advantages of polarimetry for exoplanet detection and characterization, several polarimeters are being used, built, or designed for this purpose, e.g. PlanetPol and ExPo on the William Herschel Telescope, SPHERE on the Very Large Telescope, GPI on the Gemini Telescopes, and EPICS on the European Extremely Large Telescope. It is critical to take polarimetry into account when designing and building a telescope and instrumentation, because the response of most optical components depends on the state of polarization of the incoming light: they are polarization sensitive. A polarization sensitive telescope and instrument can yield significant errors in the measured fluxes across the continuum and across absorption bands (which will influence the retrieval of gas mixing ratios).

References

Ford, E., et al., 2001, Nature, 412, 885
Fortney, J.J., et al., 2007, ApJ, 659, 1661

Hansen, J.E., & Hovenier, J.W., 1974, J. Atmos. Sci., 31, 1137
Hearty, T., et al., 2009, ApJ, in press
Karkoschka, E., 1998, Icarus, 133
Lovelock, J., 1979, “Gaia: A new look at life on Earth”, publ. Oxford University Press
Oakley, P., Cash, W., & Turnbull, M., 2008, Proc. of SPIE, 7010
Oakley, P. & Cash, W., 2009, ApJ, submitted
Palle, E.B., et al., 2008, ApJ, 676, 1319
Sotin, C., Grasset O. & Mocquet M., 2007, 191, 337
Stam, D., et al., 2004, A&A, 428, 633
Tinetti, G., et al., 2006, Astrobiology, 6
Valencia, D., O'Connell, R. J., & Sasselov, D., 2006, Icarus, 181, 545
Williams, D. M. & Gaidos, E., 2007, Icarus 195, 927-937

2.1.2 The problem of exozodiacal light

Disks of tenuous dust surround even mature planetary systems like our own. In the Solar System, the zodiacal dust is produced by collisions among asteroids, with a small contribution from comets. Similar dust also produced from collisions between and evaporation of planetesimals (asteroids and comets) is seen at much higher levels around many nearby main sequence stars. These systems were first discovered in 1984 and are now generally called debris disks (Gillett 1986). A coronagraphic image of one of the best-studied debris disks, around the nearby star Fomalhaut, is shown in Figure 1. In this case, the optical wavelength light in the image is scattered off dust in a narrow ring. The morphology of this ring strongly pointed to the presence of a giant planet, which was recently imaged close to the expected location (Kalas et al. 2008).

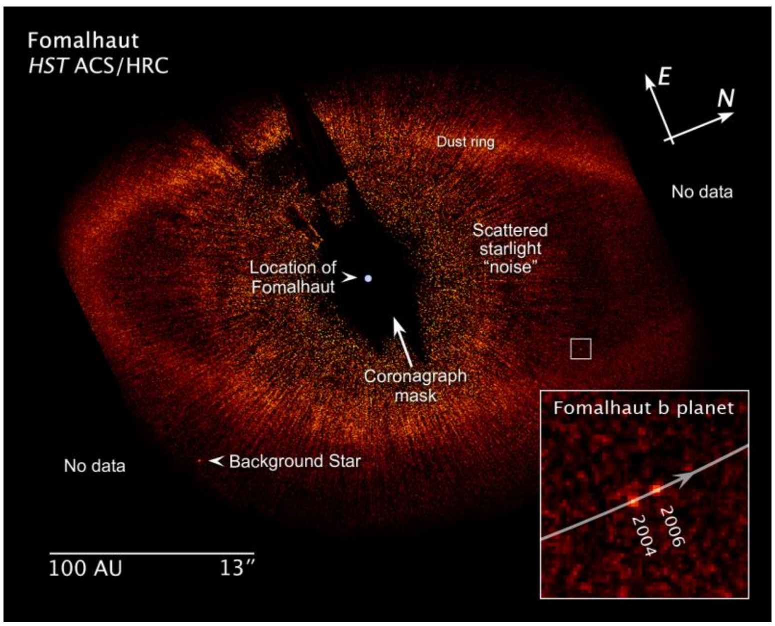

Figure 1: Direct imaging of an exoplanet in a debris disk. This optical wavelength coronagraphic image from the *Hubble Space Telescope* (*HST*) shows the debris dust ring around the nearby A3V star Fomalhaut. A possible gas giant planet is also seen (inset panel). Images taken at two epochs show that the planet candidate orbits the star. Image credit: NASA, ESA, and Z. Levay (STScI).

Debris disks are optically thin, containing modest amounts of dust, and sometimes, small amounts of gas (e.g. Roberge et al. 2006). Even the densest ones have only a few lunar masses of dust (e.g. Dent et al. 2000). These disks are found around main sequence stars with ages ranging from several Gyr to about 10 Myr, although there is tentative evidence of debris disks as young as ~ 5 Myr (Currie et al. 2008, Hernandez et al. 2008). On average, the amount of dust declines with increasing stellar age (Su et al. 2006). Observers generally quantify the amount of dust in a debris disk using the system's fractional infrared luminosity, L_{IR}/L_*, which is the light absorbed by the dust and re-emitted at IR wavelengths relative to the stellar luminosity. The currently known debris disks have L_{IR}/L_* values in the range $10^{-3} - 10^{-5}$ (e.g. Bryden et al. 2006). The zodiacal dust interior to our asteroid belt has $L_{IR}/L_* \cong 10^{-7}$; we are not currently able to detect the amount of zodiacal dust in the Solar System around other stars.

A system's fractional infrared luminosity is often given in units of "zodis." It is important to note that "one zodi" of dust simply corresponds to $L_{IR}/L_* \cong 10^{-7}$ and is not a unit of dust mass or surface brightness. The fractional infrared luminosity is proportional to the dust mass but other factors like the grain properties affect it as well. It is also important to note that although the Solar System has one zodi of dust right now, the amount of zodiacal dust has varied even over fairly recent history. Measurements of ^{3}He concentrations in seafloor sediments have shown that the amount of interplanetary dust (i.e. zodiacal dust) impacting the Earth has varied from about 0.7 to 3.3 zodis over the last roughly 80 million years, with a mean value of 1.55 zodis (Kuchner & Farley 2009). Since the zodiacal dust has such a small total mass, a single collision between asteroids, like the one that produced the Veritas family of asteroid fragments 8.2 million years ago, can temporarily but significantly raise the dust level.

Light scattered off the local zodiacal dust and the exozodiacal dust around nearby stars (exozodi, for short) is critical for efforts to image and characterize an Earth-like planet. This background flux will be mixed with the planet signal in both images and spectra. Even if nearby systems have exozodiacal dust levels no greater than the Solar System level, zodiacal and exozodiacal background will be largest source of noise for most targets, assuming that light from the central star is suppressed to give contrast of at least 10^{-10} relative to the star at the location of the habitable zone.

The exposure time required to detect a planet is proportional to the exozodi brightness. If it is too large, the integration time needed to get the desired planet signal-to-noise becomes prohibitively long. Following the approach in Brown (2005), the exposure time to image a planet in the presence of zodiacal and exozodiacal background is

$$t = \frac{2 n_x \lambda^2}{\pi F_0 \Delta\lambda D^4 T}\left(\frac{S}{N}\right)^2 10^{0.8(M_p + 5\log d - 5)}\left[\left(\frac{206265''}{1\,rad}\right)^2\left(10^{-0.4z} + \mu 10^{-0.4x}\right) + \zeta 10^{-0.4 m_*}\left(\frac{\pi D^2}{4\lambda^2}\right)\right], \tag{11}$$

where n_x = number of pixels in a critically sampled diffraction-limited image, λ = central wavelength of the image bandpass, F_0 = specific flux for zero magnitude in the bandpass, $\Delta\lambda$ = bandpass width, D = diameter of the telescope aperture, T = total facility throughput, S/N = signal-to-noise, M_p = absolute magnitude of the planet in the image bandpass, d = distance to the system in parsecs, z = surface brightness of the zodiacal dust in magnitudes arcsec^{-2}, μ = exozodi surface brightness in units of the surface brightness of one zodi of exozodiacal dust, x = surface brightness of one zodi of exozodiacal dust in magnitudes arcsec^{-2}, ζ = contrast level in the detection zone with respect to the theoretical peak of the stellar image, m_* = apparent stellar magnitude in the image bandpass, $\pi D^2/4\lambda^2$ = theoretical peak brightness of the stellar point-spread function. Typical values for these parameters appear in Table 1. For our purposes, a

“Solar System twin” has 1 zodi of exozodiacal dust with properties identical to those of the zodiacal dust.

Table 1: Typical values for the parameters in the imaging exposure time equation

Parameter	Typical Value	Explanation
n_x	1/0.08 = 12.5 pixels	Number of pixels in a critically sampled diffraction-limited image
λ	600 nm	Central wavelength of the image bandpass
F_0	9500 photons $\mathrm{sec}^{-1}\ \mathrm{cm}^{-2}\ \mathrm{nm}^{-1}$	Specific flux for zero mag in V band
$\Delta\lambda$	200 nm	Bandpass width
D	400 cm	Telescope aperture diameter
T	0.50	Estimated total throughput for NWO
S/N	10	Signal-to-noise
M_p	30	Absolute magnitude of the Earth at quadrature
d	10 parsec	Distance to system
z	23 mag arcsec^{-2}	Surface brightness of the zodiacal dust
x	22 mag arcsec^{-2}	Exozodi surface brightness for a Solar System twin (1 zodi) viewed at 60° inclination. Calculated with the ZODIPIC code (2006 TPF-C STDT Report).
ζ	2×10^{-11}	Contrast level in the detection zone relative to the theoretical peak of the stellar PSF
m_*	5.0	V magnitude of the Sun at 10 parsec

In Equation 11, the first term in the square brackets accounts for the local zodiacal background, the second accounts for the exozodi background, and the third for the residual unsuppressed stellar light. The telescope aperture diameter strongly affects the imaging exposure time, with a factor of D^{-2} for the collecting area and another factor of D^{-2} for the telescope spatial resolution, since a smaller PSF adds less zodiacal and exozodi background to the planet signal. Figure 2 shows a plot of exposure time versus exozodi brightness (μ in Equation 11), using the parameter values given in Table 1. The lines plotted give the times to get S/N = 10 on Earth-like planets in the Habitable Zones of Sun-like stars at different distances. As can be seen, the exposure time increases linearly with exozodi brightness. A useful benchmark goal is S/N = 10 on an Earth-like planet in a Solar System twin at 10 pc, viewed at 60° inclination. NWO can achieve the benchmark goal in 3.3 hours.

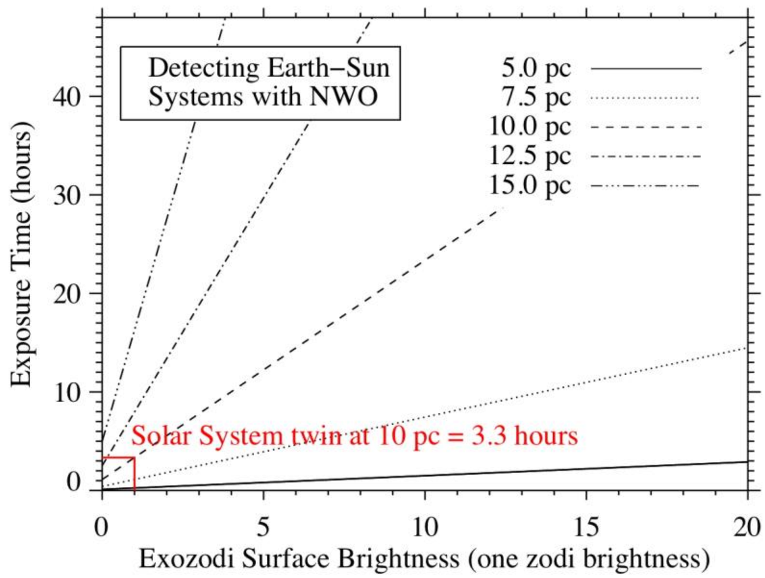

Figure 2: Planet imaging exposure time versus exozodi brightness. The y-axis shows the time to detect an Earth-like planet in the Habitable Zone at S/N = 10, calculated with Equation 11. The x-axis shows the exozodi surface brightness, in units of the surface brightness of a Solar System twin, which has 1 zodi of exozodiacal dust. The exozodi surface brightness of a Solar System twin is proportional to $10^{-0.4\,x}$, where x = 22 mag arcsec^{-2} for a system viewed at 60° inclination. The curves show the times to detect the planet around Sun-like stars at various distances between 5 pc and 15 pc. The time to detect an Earth-like planet in a Solar System twin at 10 pc is indicated in red.

Figure 2 largely serves to show the general dependence of exposure time on exozodi brightness. Figure 3 is more directly relevant to the goal of imaging exo-Earths. For this plot, we calculated exposure times to image an Earth-like planet at $S/N = 10$ with NWO for real target stars. The distance to the target star is on the x-axis. Each star is plotted as a bar showing the exposure times for exozodi surface brightnesses between $\mu = 1$ (brightness of one zodi of exozodi) and $\mu = 100$ (100 times brighter than one zodi of exozodi). Different types of stars are plotted with different colored bars.

Examination of Figure 3 highlights some interesting behavior. There are 252 and 76 targets with exposure times $\leq$ 2 days for $\mu = 1$ and $\mu = 10$, respectively. Even at $\mu = 100$, there are 79 targets with exposure times less than 20 days. For a given distance, G and K stars have shorter exposure times than A and F stars, as might have been suspected from Figure 2. If the contrast level in the Habitable Zone is fixed for all stars, fainter (later type) stars produce less residual stellar light near the planet pixel, while the planet's absolute brightness remains the same. This is slightly misleading, since the contrast level depends on the angular distance of the HZ from the star. However, the largest source of noise for most stars is the zodiacal and exozodi background, so varying the contrast level for different stars has little effect on the exposure times.

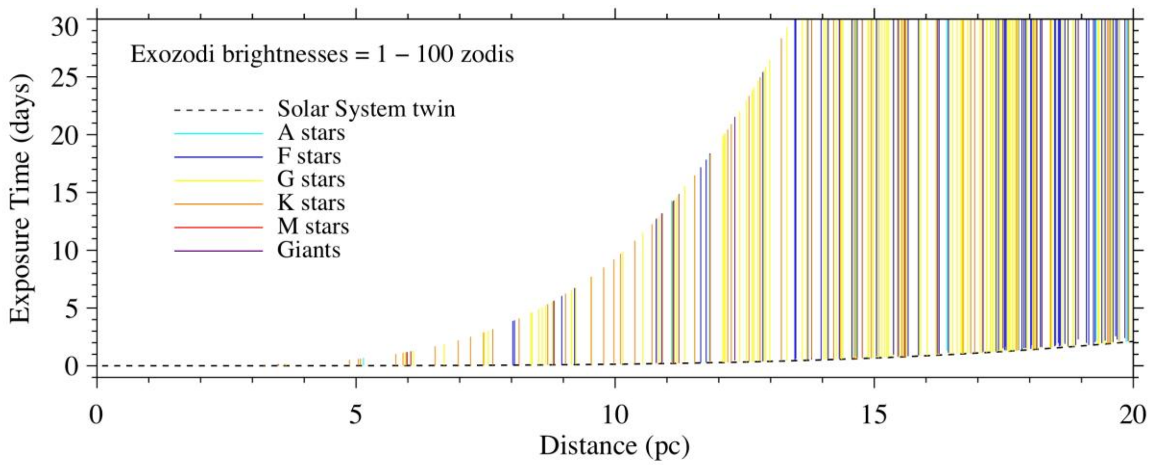

Figure 3: Planet imaging exposure time versus system distance. All times are to image an Earth-like planet at S/N = 10, using the parameters in Table 1. Each star is plotted as a bar showing the times for exozodi brightness levels between $\mu = 1$ (brightness of one zodi of exozodi) and $\mu = 100$ (100 times brighter than one zodi of exozodi). Different types of stars are plotted with different colors. The dashed line shows the time to image the Earth in a Solar System twin at various distances.

An important performance metric for an exo-Earth imaging mission is the total number of Habitable Zones searched. Figure 4 relates to this metric. Here, the NWO imaging exposure times to get $S/N = 10$ on Earth-like planets in the HZs of potential target stars are plotted versus the system completenesses calculated assuming an IWA of 50 mas. As in Figure 3, each star is plotted as a bar showing the exposure times for exozodi brightnesses between $\mu = 1$ and $\mu = 100$, with different colors for different types of stars. Given the time it takes to move the starshade, we are unlikely to spend less than about a day imaging each target. For Figure 4, the minimum imaging exposure time was set to 1 day. There are 184 stars with exposure times ≤ 2 days for $\mu = 1$ and completeness values greater than 15%. Summing the completeness values of these stars gives 82.5 total HZs. The number of expected exo-Earths imaged is the cumulative completeness times the fraction of stars with terrestrial planets in their HZ ($\eta_{\text{Hab Earth}}$).

We want to know how many Earths we can characterize in a reasonable total mission lifetime. If the total lifetime is 5 years, we can expect to use about 1 year for all the exoplanet observations, including spectroscopy as well as imaging. After 1 day of imaging, if we see a habitable planet candidate, we will immediately perform spectroscopy on it. Excluding the possibility of confusion, we can expect to do spectroscopy on ($\eta_{\text{Hab Earth}} \times 100$)% of the targets.

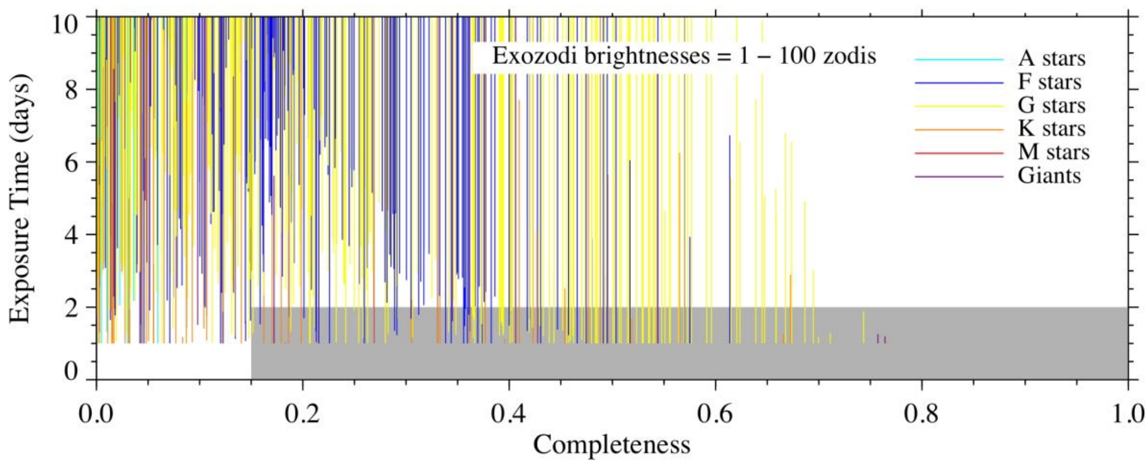

Figure 4: Planet imaging exposure time versus completeness. All times are to image an Earth-like planet at S/N = 10, using the parameters in Table 1. Each star is plotted as a bar showing the times for exozodi brightness levels between μ = 1 (brightness of one zodi of exozodi) and μ = 100 (100 times brighter than one zodi of exozodi). Different types of stars are plotted with different colors. The grey bar shows the region of the plot where $t < 2$ days and completeness > 15%.

To estimate the total program time, we need to estimate the additional time needed for planet characterization spectroscopy. The resolution of the spectrum is $R = \lambda/\Delta\lambda_{spec} = 100$. Therefore, the time needed for a spectrum with $S/N = 10$ is approximately

$$t_{spec} \approx \left(\frac{\Delta\lambda_{image}}{\Delta\lambda_{spec}}\right) \times t_{image} \approx \left(\frac{\Delta\lambda_{image}}{\lambda/R}\right) \times t_{image} \approx \left(\frac{200\ nm}{600\ nm/100}\right) \times t_{image} \approx 33.3 \times t_{image}, \quad (12)$$

where $\Delta\lambda_{image}$ is the imaging bandpass, $\Delta\lambda_{spec}$ is the width of one resolution element in the spectrum, t_{image} is the imaging exposure time for $S/N = 10$, λ is the central wavelength of the spectrum, and R is the spectral resolution. Since the minimum imaging time was set to 1 day, a blind application of Equation 12 would give a minimum spectroscopy time of 33 days. Stars with imaging times < 1 day do not require this much time to get $S/N = 10$ spectra. However, if we have a planet candidate, we're not likely to spend 1 day imaging, then take a quick spectrum and move on. There will be some minimum spectrum S/N and exposure time needed to decide whether the candidate is a real planet or not. Further study is required to determine those values. For now, we set the minimum spectroscopy time to be 1 day. This will provide spectra with $S/N \geq 10$ for all planet candidates.

We will do spectroscopy on roughly ($\eta_{\text{Hab Earth}} \times$ 100)% of the targets, but we don't yet know which ones. The total time spent on spectroscopy will be approximately $\eta_{\text{Hab Earth}}$ times the total time for doing spectroscopy at every star. Therefore, the total program time for n stars, which we want to be close to 1 year, is

$$t_{total} = \sum_{n\ stars}\left(t_{image,n} + t_{spec,n}\right) \approx \left(t_{image,n} + 33.3\ \eta_{Hab.Earth} t_{image,n}\right) \quad (13)$$

To choose stars for a possible program, we assumed that all stars have the same exozodi brightness and varied it from $\mu = 1$ to $\mu = 100$ in one zodi steps. We then calculated a weight = completeness/imaging time at each exozodi brightness level for each star. At each exozodi level, stars with weights above some limit were added to the target list and the total program time calculated using Equation 13. We iterated to find the weight limits that give total program times of approximately 1 year for every exozodi level. This procedure was performed for four values of $\eta_{\mathrm{Hab\ Earth}}$ (0.1, 0.25, 0.5, and 1.0).

The results for $\eta_{\mathrm{Hab\ Earth}} = 0.25$ are displayed in Figure 5. In this case, if $\mu = 1$ for all stars, we observe 109 targets, search 55.5 total HZs, and characterize 13.9 Earths. If $\mu = 100$ for all stars, we observe 26 targets, search 16.9 total HZs, and characterize 4.2 Earths. The actual stars selected for $\eta_{\mathrm{Hab\ Earth}} = 0.25$ and $\mu = 10$ are displayed in Figure 6. Most of the selected stars are G and K stars; no M stars are chosen. The results for the other values of $\eta_{\mathrm{Hab\ Earth}}$ are given in Table 2. At present, the amount of starshade fuel limits the total number of targets to about 85. This restricts the target list only for low exozodi brightness values.

Obviously, there are several questions to answer before we can design a truly realistic optimal observing program. Probably the most important and least studied issue is the effect of confusion, which is briefly discussed in the next two paragraphs. Nevertheless, this analysis suggests that NWO can achieve its goal of finding and characterizing habitable exoplanets over a very wide range of $\eta_{\mathrm{Hab\ Earth}}$ and exozodi brightness values.

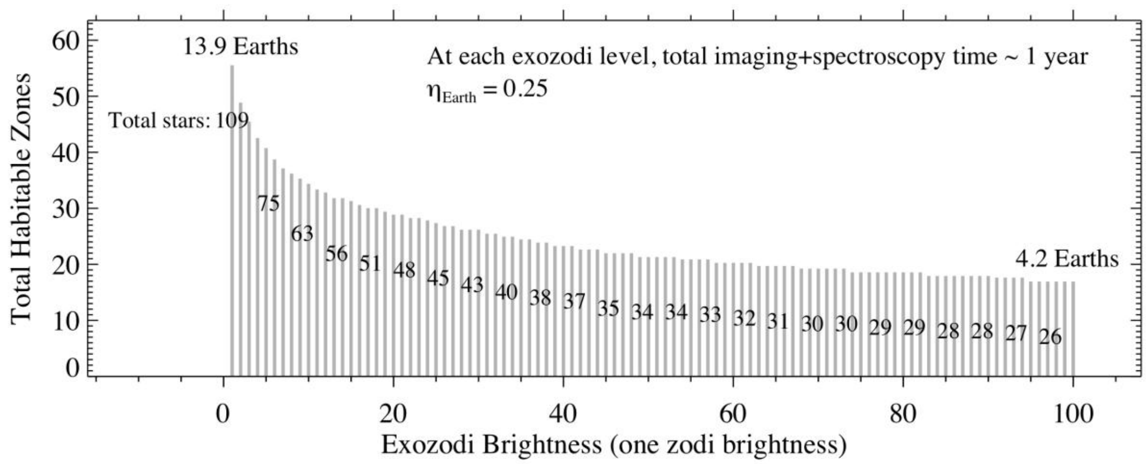

Figure 5: Total Habitable Zones searched versus exozodi brightness, assuming $\eta_{\mathrm{Hab.\ Earth}} = 0.25$. The y-axis, "Total Habitable Zones", is the cumulative completeness for all the stars observed assuming each one has the exozodi brightness given on the x-axis. For each star, we calculated 1) the exposure times for exozodi brightnesses from $\mu = 1$ to $\mu = 100$ and 2) weighting factors (completenesses / exposure times). At each exozodi level, the stars with weights greater than some limit were chosen for observation. We iterated to find the weight limits that gave total program time ~1 year at every exozodi level. The total program time was calculated assuming that for $\eta_{\mathrm{Hab.\ Earth}} \times 100 = 25\%$ of the targets, we obtain a spectrum with $S/N \geq 10$ and $R = 100$ in addition to the imaging observation. The numbers appearing on some of the grey bars are the total numbers of stars observed for various exozodi brightness levels. The total number of Earths characterized is $\eta_{\mathrm{Hab.\ Earth}}$ times the total HZs searched at each exozodi brightness level. For $\eta_{\mathrm{Hab.\ Earth}} = 0.25$, we can characterize 13.9 Earths if all stars have $\mu = 1$ and 4.2 Earths if all stars have $\mu = 100$.

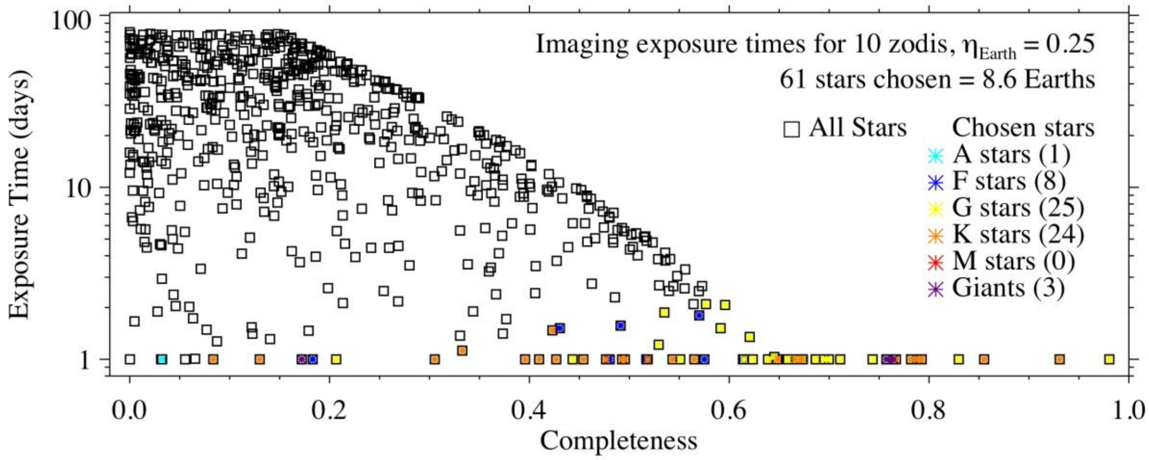

Figure 6: Stars chosen for a possible observing program. The planet imaging exposure time appears on the y-axis and the system completeness appears on the x-axis. All the potential target stars are plotted with black squares. Colored asterisks corresponding to different types of stars show the targets chosen for a possible observing program lasting 1 year (including imaging and spectroscopy). The stars were chosen using the method described in the text and in the Figure 5 caption, assuming $\eta_{Hab.\ Earth} = 0.25$ and $\mu = 10$. For each type of star, the number chosen appears in parentheses to the right of the type label. Most selected stars are G and K type; no M stars were chosen. 61 stars are observed, giving 34.4 total HZs searched and 8.6 Earths characterized.

Table 2: Total Program Results

$\eta_{Hab\ Earth}$	**Stars Observed (μ = 1, μ = 100)**	**Total HZs Searched (μ = 1, μ = 100)**	**Total Earths Characterized (μ = 1, μ = 100)**
0.10	144, 35	67.3, 22.0	6.7, 2.2
0.25	109, 26	55.5, 16.9	13.9, 4.2
0.50	88, 21	46.8, 14.3	23.4, 7.2
1.00	71, 17	39.8, 12.0	39.8, 12.0

The major outstanding problem relating to exozodiacal dust is the possibility of confusing an unresolved clump of dust for an unresolved planet. Such structures can be produced through the dynamical influence of a planet on the dust, as are the clumps of zodiacal dust leading and trailing the Earth in its orbit (Dermott et al. 1994). Since these dynamical clumps orbit the star, the possibility of confusing them with a planet in broadband images is particularly likely. In addition, an exozodiacal dust clump might be produced by a recent collision between two planetesimals or by a large comet. Dust structures, including clumps, are commonly seen in imaged debris disks (e.g. Greaves et al. 2005).

The light scattered by exozodiacal dust may not simply have the same spectrum as the central star. The zodiacal dust has a reddish scattered light color in the optical and near-IR (e.g. Matsura et al. 1995). Debris disks imaged in scattered light show a diversity of colors, from red to grey to blue (e.g. Golimowski et al. 2006, Krist et al. 2005). Nonetheless, an exozodiacal dust clump should have a featureless reflectance spectrum at optical wavelengths. A spectrum will likely allow us to easily distinguish a dust clump from a habitable exoplanet with an atmosphere. We will investigate the minimum spectrum requirements to confidently determine that an exoplanet candidate is actually a dust clump or other source of confusion. However, one does not wish to waste time taking spectra of dust clumps. It would be best to identify them using images taken in a few narrow or medium wavelength bands. We plan to study this possibility and find the optimum filter set for distinguishing between exoplanets and sources of confusion like dust clumps.

Brown, R. A, 2005, ApJ, 624, 1010-1024

Bryden, G., et al. 2006, ApJ, 636, 1098-1113

Currie, T., Kenyon, S. J., Balog, Z., et al. 2008, ApJ, 672, 558-574

Dent, W. R. F., Walker, H. J., Holland, W. S., Greaves, J. S., 2000, MNRAS, 314, 702

Dermott, S. F., Jayaraman, S., Xu, Y. L., Gustafson, B. A. S., & Liou, J. C. (1994). *Nature 369*, 719–723

Krist, J. E., et al. 2005, AJ, 129, 1008-1017

Gillett, F. C., 1986, IRAS Observations of Cool Excess Around Main Sequence Stars, In: *Light on Dark Matter. ASSL Vol. 124*, D. Reidel Publishing Co., pp. 61-69

Golimowski, D. A., et al. 2006, AJ, 131, 3109-3130

Greaves, J. S., et al. 2005, ApJ, 619, L187-L190

Hernandez, J., et al. 2008, ApJ, 686, 1195-1208

Kalas, P., et al. 2008, Science, *in press*

Kuchner, M. J. & Farley, K. A. 2009, ApJ, *submitted*

Matsura, S., Matsumoto, T., & Matsuhara, H. 1995, Icarus, 115, 199

Roberge, A., Feldman, P. D., Weinberger, A. J, Deleuil, M., & Bouret, J.-C., 2006, Nature, 441, 724-726

Su, K. Y. L. et al. 2006, ApJ, 653, 675-689

Section C: Science
Subsection C.4: Targeting and Scheduling
Lead Author: Tiffany Glassman

Problem: Given a prioritized list of desired star observations, maximize the science return for the minimum fuel. Solution: Find a near-optimal star path by performing a pseudo-random search through available star paths.

We have a list of target stars for NWO and we want to know the best order to observe them in to maximize science return and minimize mission costs. The targets are prioritized according to their completeness as described above and the science return of the mission is described by the total completeness of all the stars observed.

The mission costs are described by the Δv required for the two different types of maneuvers: retargeting and stationkeeping. We created a simple model of the circular, restricted, 3-body problem for a satellite in orbit around L2. Using the restrictions on the spacecrafts' positions and their equations of motion, we calculated the forces acting on each body and the relative acceleration between the two.

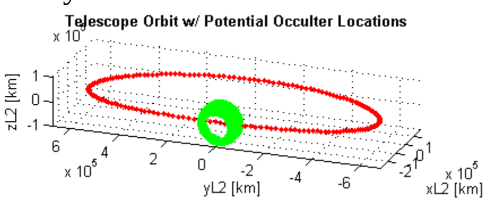

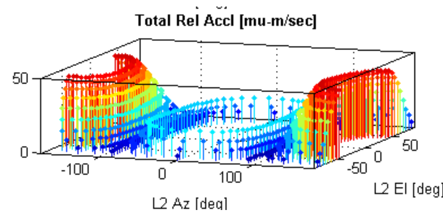

For retargeting, we calculated the optimal slew time based on the angular distance between a pair of stars. We found that the most efficient use of the starshade's time and fuel is for it to retarget at the maximum speed. This means that it would accelerate for half of the slew and then decelerate for the other half. Ground ops requires some coast time between these burns, so we left a 6 hour coasting gap in the middle of each retargeting slew. The retargeting Δv is then a linear function of the slew angle.
The relative acceleration between the two spacecraft, and therefore the Δv required to stationkeep at each star, varies with time. We must therefore calculate the stationkeeping Δv versus time for each star in order to prioritize the observations and track the total Δv used.

There are a very large number of possible paths through the target list. For 131 stars, there are 8.5e221 possible paths! A purely random search is very unlikely to find a near-optimal solution – a smart approach is needed. The time-varying Sun constraints and stationkeeping costs prevent using popular optimization schemes; you cannot simply "swap" pairs of stars to create children (genetic algorithms) or random cooling states (simulated annealing). The best approach appears to be a "wise" random search. We choose the next target star at each step according to priorities given by maximizing completeness values, minimizing retargeting angles, etc. Once we have a complete path, we rank that path using a combination of the total completeness of the stars, retargeting Δv, stationkeeping Δv, time to complete mission, etc. These constraints can be weighted differently to produce the best possible path.

The best path is run through a complete STK model of the NWO system in order to confirm the fuel needs for both types of maneuver.

Appendix C: Data Simulations and Analysis – Phil Oakley

Overview

Simulating observations from a New Worlds Observer system is critically important for several reasons. Among the many reasons are the ability to: quantify our expected science return, intelligently make design decisions (necessary throughput, bandwidth, starshade tolerancing, etc.) to maximize scientific return, create a realistic exoplanet searching / characterizing / revisit schedule, and create a potential target list.

A detailed simulation of an exoplanet observation with NWO would include accurate source functions for the star, planet and exo-zodiacal light. These sources located at their specific angular positions need to be properly convolved with both the starshade and optical system (with proper characteristics for the various mirrors, filters, detectors, etc.) to obtain a realistic NWO simulated observation.

Simulated Planetary System

For conceptual reasons we typically simulate a planetary system that is identical to our own in terms of planetary locations, radii, albedo, etc. and place it at 10 parsecs from our own. The sun is fairly straightforward to simulate as it's brightness and spectrum are well known.

The Earth's average brightness and spectrum are known from Earthshine observations (Woolf et al. (2002), Hamdani et al. (2006), Turnbull et al. (2006), Arnold et al. (2002), Montañés-Rodriguez (2006) and Seager et al. (2005)), however these can vary as a function of rotation. As different sections of Earth are observed the average brightness will change depending on the visible terrain and cloud coverage. Modeling this variation was first done by Ford et al (2001) and later by Palle et al (2008). We follow the approach of Oakley & Cash (2009) and Oakley et al (2008) as it includes dynamic snow and ice coverage maps as well as regularly updated cloud maps. The basic approach involves taking constantly updated terrain and cloud maps and calculating the locations both visible and illuminated. From this we can simulate the brightness based on the bi-directional reflectance distribution functions (Manalo-Smith et al. (1998)). With this model we can calculate Earth's brightness at any given system geometry, time of day, and day of the year (including seasonal effects) using empirical maps that can be updated on short timescales.

The last component that needed modeling was the brightness and distribution of exozodiacal dust. This was accomplished by using the zodiacal dust modeling software: Zodipic (Moran et al. (2004)). This uses observational data to model our zodiacal dust. Exo-zodiacal light could vary substantially from our own, but the first logical step is to model our own zodiacal distribution.

Simulated New Worlds Observer Response

After creating our observed planetary system we then had to properly convolve it with an NWO response. This includes both the starshade and the telescope. The starshade response was calculated based on the techniques in Cash (2001). This includes a response that varies as a function of the planet's angular distance from the center of the starshade as well as wavelength. The starshade parameters vary throughout different studies, but for the simulations below we use a 50 meter starshade with a 4 meter telescope.

The next step is to follow the image through the actual telescope. The telescope's mirrors are taken to be diffraction limited over the optical bandpass. The efficiencies and bandpass (i.e. filters or dichroics) are varied to test different configurations, but are generally set to ~50-80% throughput followed by the typical bandpass of modern filters. Detectors are assumed to have Q.E. and noise levels (dark noise and read noise) comparable to current CCDs.

Analysis of Simulated Images

The end result of a single simulated image is the detection of planet(s) above the noise from diffracted and exo-zodiacal light to some level of significance. From the location of these planets we can begin to deduce planetary locations and orbits that will reveal whether they are likely in the habitable zone of the system. Confirmation of this will require multiple visits, but statistical probabilities will give us a preliminary indication depending on the geometrical complexity of the system. Additionally, exozodiacal light can give us an immediate tool for determining the system inclination. An example of this is shown in Figure 1. This initial orbital determination will help guide us towards the need and timing for a return visit with the starshade. This figure epitomizes the usefulness of the exo-zodiacal dust and should make clear the importance of an observing system that can image the distribution.

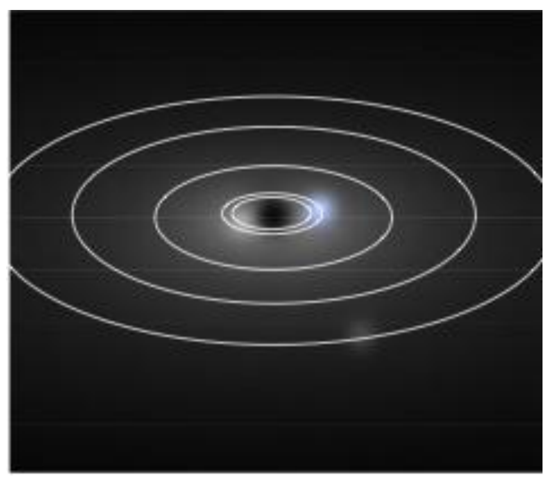

Figure 1: Light contours of exo-zodiacal light can help determine the inclination of the planetary system, thus giving us a powerful tool for orbit determination.

Spectral analysis will provide a wealth of information about atmospheric constituents, including potential biomakers such as water and oxygen. For example, simple color analysis on Earth using standard filters produces the results in Figure 2. The complete disappearance of the planet in the ozone band is strong evidence of oxygen in the atmosphere. Color analysis can be achieved in a few relatively short exposures, and can be a powerful diagnostic tool. Spectral analysis is covered in more detail in other sections of this document.

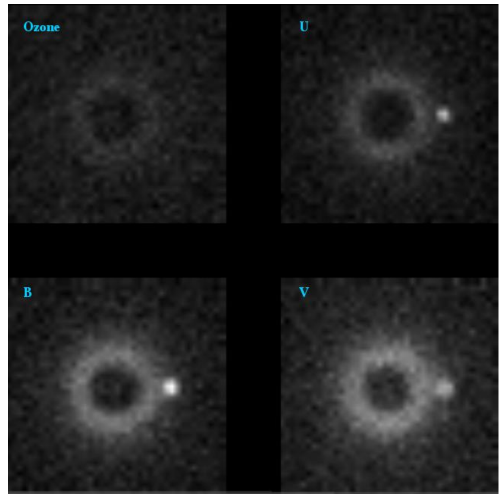

Figure 2: Image of our solar system through NWO using standard UBV Johnson filters and a bandpass in the Ozone absorption band.

An additional, and exciting, branch of analysis involves monitoring the temporal variation in planetary brightness. As mentioned above, our planetary model incorporates the instantaneous surface terrain and cloud coverage for any given observational geometry and orbital location. Thus we can advance our observations in time and watch the planet fluctuate in brightness. These fluctuations are caused by changing cloud cover, changing visible terrain, changes in the terrain at any given location (i.e. snow in the winter) and specular reflection off of smooth features. An example of this is shown in Figure 3.

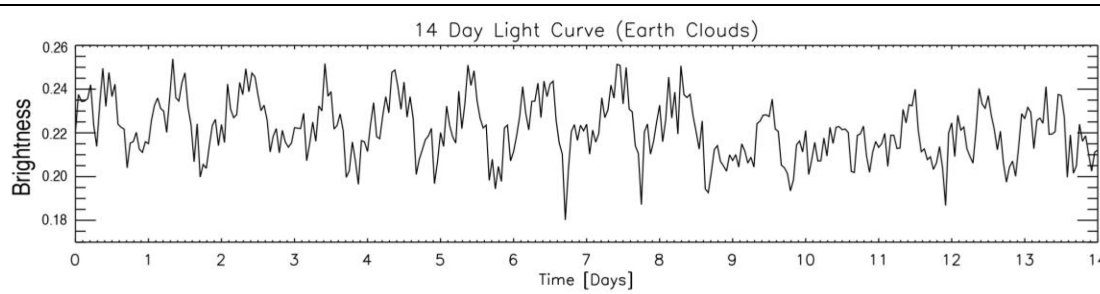

Figure 3: Sample data over 14 days of observation. The hourly variation is due to the changing disk-averaged albedo of the planet as clouds and surface features rotate into view. Given sufficient observation time the rotation rate of the planet can be accurately determined.

A repeated pattern in the planetary brightness is clearly discernable in the simulated data. This is primarily due to cloud structures, but also to the pattern of surface terrain. From this data it is fairly straightforward to determine the rotation rate of the planet. Analysis of this type of data shows that we can accurately determine the rotation rate at a success rate above 50% given observations with a SNR ~5-10. This type of analysis is detailed in Oakley & Cash (2009) and Palle et al. (2008). There is also potential for determination of the presence of surface water via the intense specular peaks visible during crescent phases. This analysis is difficult due to the dimmer planetary phase, but may be possible for nearby systems with relatively low levels of exo-zodiacal light.

We now have a tool that can simulate an NWO observation with a planetary system using any parameters of our choice. This tool can incorporate the starshade parameters (size, distance) as well as telescope characteristics (size, throughput, noise, etc.). This tool can be used for design tradeoff decisions, target choices, determination of revisit cadences as well as quantifying our expected science return.

References

Arnold, L., Gillet, S., Lardiere, O., Riaud, P., & Schneider, J. 2002, A&A, 392, 231

Cash, W. 2006, Nature, 442, 51

Ford, E.B., Seager, S., & Turner, E.L. 2001, Nature, 412, 885

Hamdani, S., et al. 2006, A&A, 460, 617

Manalo-Smith, N., Smith, G.L., Tiwari, S.N., & Staylor, W.F. 1998, JGR, 103, 19733

Montanes-Rodriguez, P., Palle, E., Goode, P.R., & Martin-Torres, F.J. 2006, ApJ, 651, 544

Moran, S. M., Kuchner, M. J., & Holman, M. J. 2004, ApJ, 612, 1163

Oakley, P., Cash, W., & Turnbull, M. 2008, Proc. SPIE, 7010

Oakley, P.H.H., Cash, W., 2009, submitted

Palle, E., Ford, E.B., Seager, S., Montanes-Rodriguez, P., & Vazquez, M. 2008, ApJ, 676, 1319

Seager, S., Turner, E.L., Schafer, J., & Ford, E.B. 2005, Astrobiology, 5, 372

Turnbull, M.C., Traub, W.A., Jucks, K.W., Woolf, N.J., Meyer, M.R., Gorlova, N., Skrutskie, M.F., & Wilson, J.C. 2006, ApJ, 644, 551

Woolf, N.J., Smith, P.S., Traub, W.A., & Jucks, K.W. 2002, ApJ, 574, 430

General Astrophysics with New Worlds Observer

John Bally
CASA, University of Colorado, Boulder

Abstract

New Worlds Observer (NWO), a 4-meter class telescope designed to detect and characterize Earth-like planets around nearby stars with a star-shade, will be a powerful observatory for general astrophysics (GA). NWO will have extended UV and near-IR sensitivity, angular resolution nearly a factor of two better than Hubble or JWST, and unprecedented astrometric and photometric stability due to its high Earth orbit. Wide-field focal-plane array imaging conducted in parallel with star-shade assisted exo-planet observations will find background planets around field stars using transits and gravitational micro-lensing. Deep synoptic monitoring of these fields will detect distant supernovae, some of Type Ia, which can be used to measure cosmic acceleration and the properties of dark energy. These data will set stringent new constrains on all types of variable and moving sources including comets, asteroids, variable stars, and GRB after-glows in the fields surrounding every NWO target star. The time-averaged data will enable mapping of the distribution of dark matter in distant galaxy clusters using the "weak-lensing" method of searching for correlations in gravitationally lensed galaxy shapes. While the star-shade is being moved to a new target, the NWO 4-meter telescope can be used for general astrophysics observations including spectroscopy of targets requiring precise pointing. Over half of NWO space-craft hours will be available for general astrophysics, enabling investigations being proposed for other, dedicated, but smaller space telescopes.

A 4 m Telescope for General Astrophysics

A 4 meter class space telescope in a high-Earth orbit such a Lunar Halo L2 is a technologically mature concept that can be realistically developed and flown during the next decade. It provides an order of magnitude improvement over HST in point source sensitivity. Equipped with large focal plane arrays, spectrographs, and instrumentation optimized for astrometry, a 4 meter diameter facility can conduct most of the science investigations being proposed for the next decade in the ultraviolet to near-infrared spectral domains. The prime science goals for a 4 meter New Worlds Observer and associated star-shade are the detection and characterization of Earth-like extra-Solar planets. However a properly equipped NWO will also serve as a general purpose observatory that will address the major astrophysical challenges of the next decade.

The "general astrophysics" potential of NWO can be sub-divided into four categories: (1) indirect exo-planet searches using transits and lensing. (2) The origin, evolution, and demise of stellar and planetary systems. (3) Coordinated deep synoptic surveys for variable sources such as SNe, GRBs suitable for mapping the distribution of dark matter and the evolution of dark energy. (4) Galactic and extra-galactic astronomy and cosmology to measure the cosmic evolution of ordinary matter.

The LHL2O enables precision photometry and astrometry. Based on the expectations of the Kepler mission, precision photometry to 1 part per 10^5 should be possible. Furthermore, the thermal environment implies a stable geometry for the focal plane, implying precision relative astrometry. Photometry enables exo-planets searches using gravitational lensing and transits, and the measurement of the properties of dark energy using supernovae. Precision relative astrometry will enable the mapping of dark matter distributions using the correlation of observed galaxy shapes, and the determinations of proper motions and parallaxes of stars, planets, and other nearby objects.

General Astrophysics (GA) projects to be conducted with a 4 meter NWO include:

- Indirect searches for extra-Solar planets by means of transits, gravitational micro-lensing, and astrometry.
- Probing the distant Universe by searching for and analyzing the light of distant supernovae (SNe) and gamma-ray bursts (GRBs)
- Investigation of the cosmic evolution of galaxies and galaxy clusters.
- Tracing the cosmic evolution of dark energy.
- Mapping the distribution of dark matter.
- Characterization of the stellar populations of the Milky Way and Local Group Galaxies.
- Probing the cradle-to-grave evolution of stars and planetary systems of all masses.
- The analysis of the “Galactic Ecology”, the cycling og the ISM from stars back to the ISM using UV, visual, and near-IR tracers.

General Astrophysics observations can be conducted both during planet finding and characterization (parallel observations), and while the star-shade and NWO are being re-configured for the observation of another target (stand-alone mode). While the NWO 4 meter is observing a nearby target star being occulted by the star-shade, the wide-field camera can be used to obtain deep images of the background field.

When NWO targets *high Galactic latitude fields*, the background will primarily consist of distant galaxies. Deep imaging of these fields will be used map the distribution of dark matter using the distortions of galaxy images produced by weak gravitational lensing of the dark matter (Tyson et al. 1990; Fischer et al. 2000). They will also be analyzed for transient events such as supernovae and GRBs. The Type Ia SNe will be used to map the evolution of cosmic deceleration and acceleration and the resulting equation of state of dark energy (Riess et al. 1998; Perlmutter, S. 1999). The insertion of grisms or other dispersing elements into the focal plane can facilitate the identification the supernova type.

When NWO targets *low Galactic latitude fields*, the background will primarily consist of stars. Deep imaging and photometry will characterize the stellar populations along these lines-of-sight. Synoptic monitoring of these fields will identify all variable stars along the line of sight. This data will be used to find extra-Solar planets by means of two indirect planet detection techniques; planetary transits (e.g. Sato et al. 2005) and gravitational micro-lensing (Beaulieu et al. 2006).

While NWO and the star-shade are being re-configured for the observation of a new target star, repeated visits to the fields surrounding target star without them being occulted by the star shade will be used to optimize the time sampling of synoptic programs. Additionally, such time will be used to observe specific targets such as Galactic star forming regions, nearby galaxies, and targets chosen for spectroscopy. Re-configuration time cal also be used to support a health general guest observer program to which members of the science community can apply in an open competition. Over 50% of the telescope time on NWO will be available for GA programs.

The 4 meter aperture of the NWO telescope will out-perform 2 meter class facilities being considered for conducting missions dedicated to specific science goals such as mapping dark matter, tracing dark energy, probing star formation in the local Universe, or finding extra-Solar planets by means of micro-lensing or transits. In the diffraction limit, the point-source sensitivity increases as telescope diameter to the fourth power (the diffraction spot size decreases as D^2 and the amount of light put into the spot increases as D^2 , resulting in a signal / noise gain proportional to D^4 in the presence of a diffuse background or detector noise). Thus, each of the major science objectives can me met by NWO in a small fraction of the time required from a smaller aperture. For some projects such as dark matter mapping using weak lensing, the smaller diffraction spot-size greatly increases precision and speed. For point source detections such as SNe or GRBs, a 4 meter telescope provides a 16-fold increase in detection speed. The advantage of NWO for the detection of planets using transits and microlensing may be smaller since NWO will only be able to stare at a given star field for a fraction of the time. Nevertheless, the timing of observations can be optimized for specific types of target such as planets in close in, “hot” orbits, or Earth-like planets around G-stars that require a transit cadence of about 1 year.

Instrumentation Requirements for General Astrophysics: The General Astrophysics Instrumentation Suite

A 4 meter diameter, wide-field OTA. A 4 meter aperture can be fabricated and launched without the requiring on-orbit assembly. Such an aperture in high Earth-orbit, optimized for $\lambda = 0.2$ to 3 μm will provide an order of magnitude improvement in resolution and sensitivity over the Hubble Space Telescope. Yet, the deployment of such an aperture is not as daunting as a larger one; the development, design, and launch of a 4 meter OTA does not require the development of any new technology or deployment approach. Such a facility can be developed, build, and launched during the next decade with minimum risk and well defined costs.

NWO will be a powerful general purpose 4-meter class space observatory that can conduct many of the science investigations being proposed for dedicated missions during the next decade. General astrophysics can be conducted in parallel with coronagraphic imaging of planetary systems around nearby stars by acquiring images with its wide-field camera, and while the star-shade is being moved to the next target. A D = 4-meter diameter telescope can deliver diffraction limited images with a resolution q = l / D = 0.01 arcseconds (10 milli-arcseconds or 10 mas) at l = 0.2 mm or 50 mas at l = 1.0 mm. Nyquist sampling would imply a 5 to 25 mas pixel pitch at these wavelengths. Operations in a lunar halo L2 orbit (LHL2O) implies a stable thermal and dynamic environment that will permit precision photometry and relative astrometry.

A wide-field imaging array. With current technology, a minimum of 65 Mpixels (8192 x 8192 pix should be considered (this is 4 x ACS). However, pixel counts as large as 10^9 pixels, multiple pixel scales, and sensors that work into the near-IR as well as the near-UV should be evaluated and considered. A filter set comparable to that being installed on HST WFC3 should be considered. Wavelength coverage extending from the near-UV (1,500 A to about 3,000 A), through the visual (3,000 to about 8,000 A), and near-IR (8,000 A to about 3 μm) should be considered. The broad-band coverage can be best achieved using dichroic splitters so that the pixel-scale in each band can be matched to the diffraction spot size. Extension to about $\lambda = 3$ μm is highly desirable to provide overlap with the capabilities of JWST. Extension into the near-UV is needed since beyond HST, there are no currently envisioned large-aperture UV missions. The lower-cutoff should be determined by the cost-benefit of avoiding exotic UV-optimized coatings.

To accommodate the large wavelength and resolution range of NWO, several different pixel-scales (pitches) ought to be considered. For 10 mas pixels, a 1 square arcminute field implies 2.6×10^7 pixels and a 10'x10' field implies 3.6×10^9 pixels. Thus, the pixels counts and implied space-to-ground downlink bandwidths are huge. Either on-board image processing and data compression, or a laser communications link to the ground ought to be considered. The filter wheels should carry grisms suitable for the rapid characterization of transient and flaring objects without the need to place the target in the spectrograph aperture.

The limiting factor on array size and pixel count is likely to be the data downlink bandwidth. Instead of traditional radio links using DSN or dedicated radio dishes, alternative communications technologies should be explored. These include: [1] An optical laser link that utilizes a conventional optical telescopes as receiver / transmitter pairs both on the spacecraft and on the ground. 10 to 100 Gbits/second are feasible with such links. [2] A millimeter or sub-millimeter link using frequencies above 70 GHz. Above 300 GHz, FCC regulations of the radio spectrum end so a sub-mm communications link could support large focal-lane arrays. However the receiver antenna would need to be located on a high and dry mountain site.

A general purpose UV/ VIS/ NIR spectrograph. A spectrograph having long-slit, and multi-slit capability with a resolution of at least 10^4 should be considered. UV sensitivity is especially important as this is unique regime not accessible from the ground. Desirable capabilities include a long-slit mode, a tunable multi-aperture mode for the simultaneous recording of the spectra of sparsely distributed targets, and a dense-pack integral-field mode optimized for the recording of 3D data cubes over small fields of view for the study of the kinematics and excitation conditions in extended objects. A multi-arm spectrograph design could enable the recoding of spectra over the entire functional wavelength range of NWO. Coverage of the UV and near-IR bands is especially important as there is little or no ground-based capability. In the UV there are no large-aperture telescope being contemplated, and in the near-IR, airglow severely limits sensitivity. In the visual, NWO provides unique access to high-contrast diffraction limited spectro-imaging over wide fields of view.

Deep-space operations also will enable unique far-UV spectroscopy with diminished geo-coronal Lyman alpha backgrounds. Thus a UV-capable spectrograph should also be flown. The spectrograph, properly designed, can also serve as the exo-planet characterizer.

A high-contrast-ratio astrometer: A prism block that dices-up the light of a bright star (magnitude 3 to 10) into an array that can be superimposed on a wide-field background of faint stars and galaxies with magnitudes of 15 to 25 will enable precision astrometry of the planetary search target stars. This is essential for the determination of planetary orbits and masses. Astrometric precision of 1 to 10 micro-arcseconds should be attainable (see Appendix 4).

The stable thermal and mechanically quiet environment of a high-Earth orbit will enable the determination of the centroids of images to a precision ranging from 10^{-2} to 10^{-4} of the diffraction limited image diameter (the exact value depends strongly on the signal-to-noise in the image). Differential astrometry across the field-of view can approach 1 micro-arcsecond if suitable provisions are made for the mechanical stability of the detector and optical train.

Summary

A suitably equipped 4-meter class NWO can achieve most of the science goals of the major space astrophysics missions being proposed for the second decade of the 21-st century, including the search and characterization of terrestrial exo-planets, the formation and evolution of galaxies, stars, and planetary systems, the mapping of dark matter, and the characterization of dark energy. Additionally, a substantial amount of time will be available for a guest observer program that solicits observing proposals from the community.

References:

Beaulieu, J, P. et al, 2006, Nature, 439, 437
Fischer, P. et al. 2000 , AJ, 120, 1198
Perlmutter, S. et al. 1999, ApJ, 517, 565
Reipurth, B. & Bally, J. 2001, Ann.Rev.Astro.Astrophys., 39, 403
Riess, A. g. et al. 1998, AJ, 116, 1009
Sato, B. et al. 2005, ApJ, 633, 465
Throop, H. & Bally, J. 2005, ApJ, 623, L149

Tyson, J.A., Valdes, F., & Wenk, R.A. 1990, ApJ, 349, L1
Walawender, J., Bally, J, & Reipurth, B. 2005, AJ, 129, 2308

Appendix 1: Planet Formation and Evolution

Much of the general astrophysics to be conducted with NWO will strengthen the connection between NWO's primary mission of planet finding and characterization and the rest of astrophysics. Specifically, the study of nearby, Galactic star forming regions, stellar populations, and post-main sequence objects such as planetary nebulae, supernovae, and stellar remnants will inform our understanding of the birth, evolution, and destruction of planetary systems. Such studies will shed light on the diversity of planetary architectures, the abundance and habitability or Earth-like planets, and fate of planetary systems as their central stars evolve towards the stellar graveyard.

The detection various components of the outer planetary systems surrounding nearby stars will shed much light on the evolution and architectures of planetary systems. Additionally, the study star formation regions within about 1 kpc of the Sun using the General Astrophysics Instrumentation Suite will inform our views on the formation of such systems. The detection, characterization, and orbit determinations of nearby gas- and ice-giants in the outer parts of planetary systems will provide important clues about the long-term dynamical evolution of planetary systems. Are most outer giant planets (beyond a few AU where our current knowledge is very poor) in circular or eccentric orbits? Are mutual perturbations to planetary orbits common or rare? Are the eccentricities generated by interactions damped efficiently by swarms of small bodies, or do they survive for billions of years? Answers to these questions will profoundly impact the potential habitability of terrestrial planets in the habitable zones of the host stars.

The Hubble Space Telescope studies of the Orion Nebula has profoundly altered our view of planet formation. We have learned that most planetary systems form in rich clusters containing dozens to thousands of stars. In small clusters and groups, protostellar outflows and winds regulate the properties of the environment (Reipurth & Bally 2001; Walawender et al 2005). In the larger clusters, massive stars dominate evolution of the star-forming environment. Their UV radiation photo-ablates disks, limiting the amount of time available for planet formation. But, photo-ablation may also promote the growth of planetisimals, thereby speeding up the process (Throop & Bally 2005). In the standard model of gas-giant formation, a large "super-Earth" sized cores form, followed by the run-away accretion of hydrogen and helium. But, in UV-rich HII regions, disks lose hydrogen rapidly. Thus, core formation followed by accretion must occur faster than gas removal, otherwise the resulting planetary system will lack gas (and ice) giants.

NWO will constrain these processes by (1) providing reliable statistics on the presence of ice and gas giants in long-period orbits in mature planetary systems, and (2) provide estimates of disk lifetimes and UV-induced mass-loss rates in a number of star forming environments. The wide-field imager, spectrograph, and a conventional internal coronagraph will facilitate many of these studies.

Observations of star and planet forming regions can be conducted with NWO while the star-shade is being moved from target to target. Such studies will inform our understanding of the formation and early evolution of planetary systems and the great diversity of planetary system architectures.   Near-UV, visual, and near-IR imaging and spectroscopy of star forming regions within a few kpc of the Sun will probe the earliest phases of star and planet formation where UV radiation fields have stripped away obscuring material. The high angular resolution of a 4 meter telescope will be used to study disk structure and evolution, the launch and collimation of stellar jets, and the roles of massive stars and siblings in the formation and early evolution of planetary systems. Studies of older stellar clusters and associations will enable NWO to bridge the time from planetary birth to the mature nearby planetary systems being characterized with the star-shade. It will thus constrain the formation time-scale for planetary systems as a function of their architecture and environment.

Appendix 2. Indirect Exo-Planet Searches:
Transits, Gravitational nano-Lensing, and Astrometry

A large FPA surrounding the planet imaging sensor can be used to search for planets using two indirect methods; transits and gravitational microlensing.   While NWO and the star-shade are imaging the circumstellar environs of nearby stars, the surrounding star-field can be continuously imaged with the FPA.   A cadence of order few minutes per frame can be used to search for planetary transits.   Co-additions of data to achieve a cadence of a few hours can be used to search for stellar micro-lensing events. The short-cadence observations can then be used to search for the short-duration “nano”-lensing signatures of planets orbiting within a few-AU of the lensing stars.   The mass sensitivity and duration of gravitational lensing scales as the square-root of the lens mass. Stars typically produce time-symmetric (about peak light) and achromatic lensing signatures lasting a few weeks. Jovian planetary lensing events last about a day, terrestrial planets last about 1 hour, and lunar mass objects amplify the light of the background star for about 10 minutes. The MACHO and OGLE projects have shown that the “optical depth” of stellar micro-lensing events is about 10^{-7}, implying that any one time one star out of 10^{7} will undergo a lensing event at any one time.

The Kepler mission will serve as a pathfinder for the rate of planetary transit events in one specific star field. NWO will enable the transit rate to be determined towards dozens of other lines-of-sight.   Its larger aperture will enable transit searches to fainter magnitudes than Kepler.

The differential astrometer described below can be used to search nearby stars for massive planets by stellar astrometry. It can also be used to determine the exact location of each NWO target star before and after imaging of its planetary system with the star-shade. Stellar astrometry referenced to background stars and galaxies, combined with deep imaging of the circumstellar field will enable the determination of the orbit of each planet with respect to its central star. Several epochs of astrometry can then be combined to determine planetary masses directly.

Appendix 3: Deep Synoptic Surveys

Parallel (with exo-planet imaging and characterization) FPA observations can also be used for distant high-z supernova searches and other synoptic monitoring programs. High-latitude star fields surrounding NWO target stars will be imaged for periods of days to weeks. These images will provide some of the deepest images of the extra-galactic background ever obtained. They can be used to search for transients such as supernovae and flashes caused by events such as gamma-ray bursts. The subset of type 1a supernovae (SN) can be used to trace cosmic deceleration due to gravity at early cosmic times and acceleration due to dark energy in recent times, thereby providing constraints on the equation of state of dark energy. Thus, NWO can accomplish the mission goals of JDEM. Type II SN will be used to trace massive star-formation in the early Universe; NWO will compliment the JWST mission. The 4 meter NWO aperture will provide the sharpest images of galaxies, enabling the study of galaxy morphological evolution over cosmic time. Correlations of galaxy shapes can be used to map the distribution of dark matter using gravitational lensing in the "weak-lensing" limit.

Deep images of low-galactic latitude star fields will be used to investigate the full range of stellar photometric variability including eclipsing binaries, variable stars, and stellar oscillations, and as described above, to search for planetary systems. The various fields being investigated during NWO's main mission can be re-visited while the starshade is moved to the next target star. Thus, the cadence of synoptic imaging can be optimized for the identification and follow-up of various categories of variable object. Most fields can thus be monitored for the lifetime of the NWO mission.

Appendix 4: A Differential Astrometer

The image dicer consists of a solid prismatic block that slices the image of the bright star into a regular grid and diminishes is apparent brightness so that it is comparable to the brightness of the dim astrometric reference objects.

Figures 1 – 4 show one possible scheme. Figure 1 shows a prism-block that can be used to dice an image in 1 dimension. Figure 2 shows how a stack of such dicing prisms can be used to generate a 2D grid of images. Figure 3 show the desired focal plane geometry. Figure 4 shows a possible scheme for superimposing the diced images of a bright star onto an image of the surrounding star field.

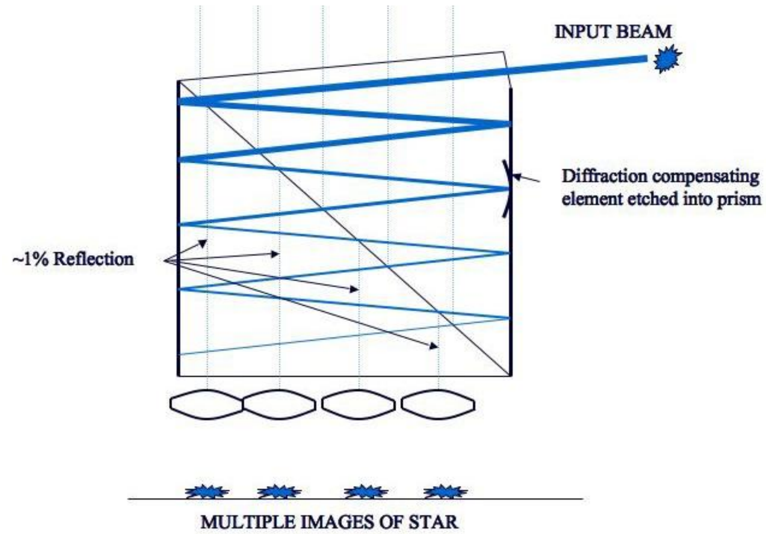

Figure 1: A prism block that can make multiple copies of the image of a bright star. The increasing path length can be compensated by a corrective optic polished into the face of the prism.

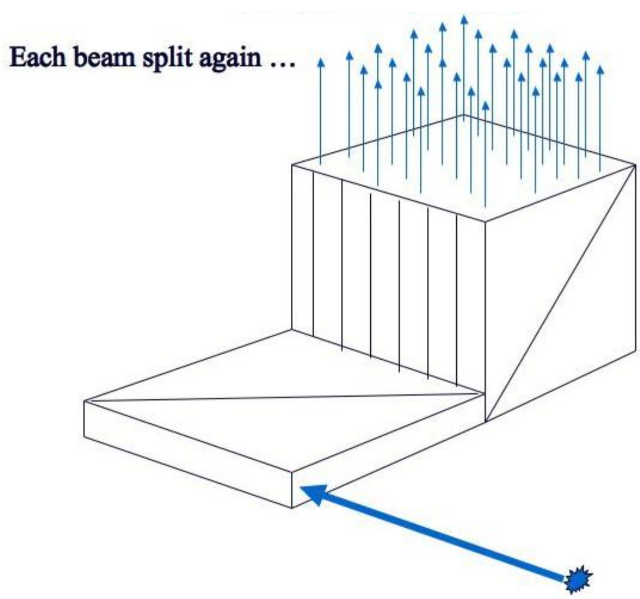

Figure 2: Each output of the first prism is dissected further by a prism oriented orthogonal to the first. The output consists of a uniform grid of images of the input field that is highly attenuated in brightness.

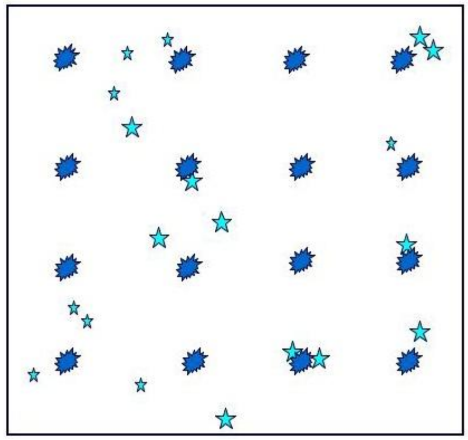

Figure 3: The focal plane geometry. Blue stars represent the output of the image dicer. Turquoise stars represent astrometric reference objects (stars or galaxies) in the field surrounding the target star.

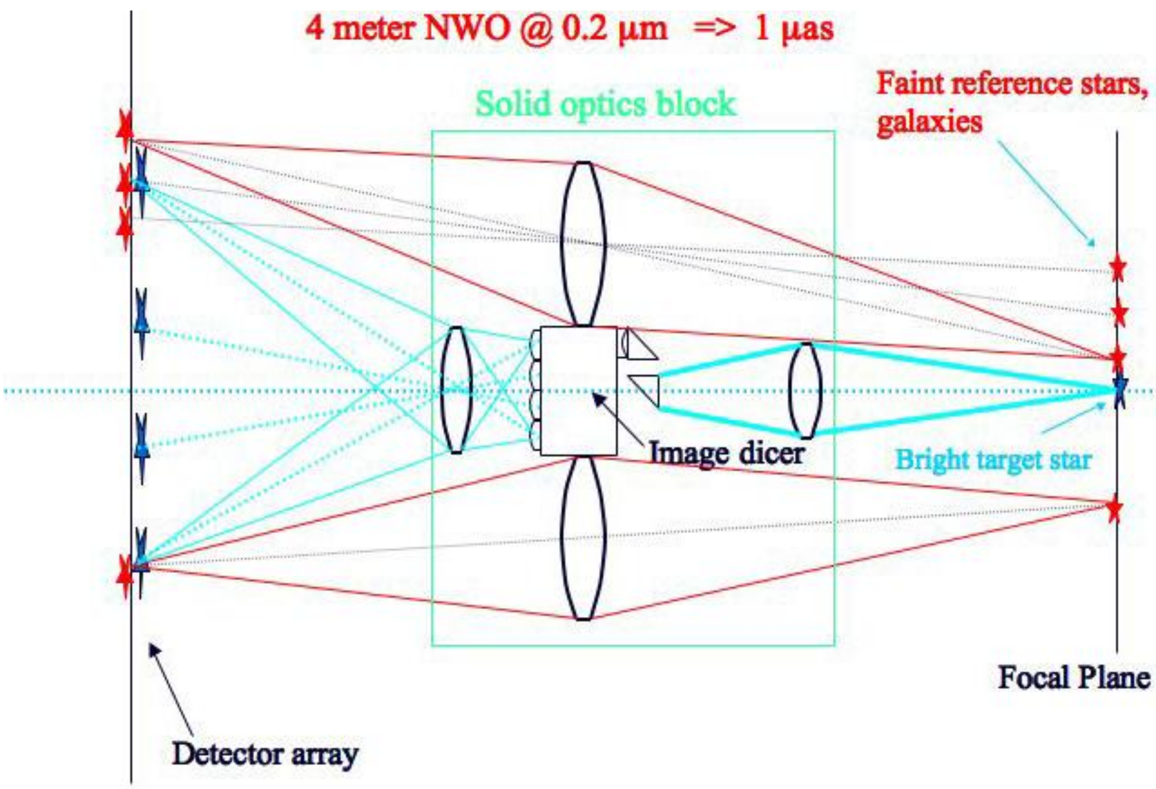

Figure 4: A possible implementation of the differential astrometer. The NWO focal plane is shown on the right. Reference stars and galaxies are shown in red. These objects are re-images onto the detector array on the left by the lenses mounted on the image dicer. In practice, these lenses might consist of an all reflecting Offner relay. The bright target star is shown in blue. Its image is diced into a regular grid by the image dicer. The grid of images output of the dicer is imaged onto the detector array. A partially reflecting surface located behind the Focal Plane can be used to inject images of artificial stars to calibrate and monitor the geometry of the astrometer.

New Worlds Observer
Astrophysics Strategic Mission Concept Study

APPENDIX C.7
ASTROMETRIC DETECTION OF PLANETS USING THE NEW WORLDS OBSERVER

This is a paper written by members of the New Worlds team at the US Naval Observatory. They looked at the use of the 4m telescope as defined in the concept study to perform astrometry on the target stars. They conclude that many exoplanets can be detected astrometrically, although true Earth-twins are likely just beyond the reach of NWO through this approach.

Astrometric Detection of Planets with NWO

R. P. Dudik and B. N. Dorland
U. S. Naval Observatory

Abstract

We present an astrometric analysis examining the planet detection capabilities of a New Worlds Observer-class telescope. We find that for a 5-10 year mission lifetime, Jupiter-mass gas giant planets with large orbital radii can be detected out to 1-kilo-parsec, so-called "Super-Earth" rocky planets with masses up to 10 Earth mass can be detected beyond the habitable zone out to 50 pc, and Earth-mass planets beyond the habitable zone can be detected at a distance of up to 5 pc for late-type, low mass stars. Detection of these so-called "cold Jupiters" are critical for selecting and screening targets for potential follow-up with alternate instrumentation, as they are thought to be markers of systems most likely to host habitable Earth-type planets. We examine the capability for astrometric detection of habitable planets around nearby stars. While astrometric detection of habitable Earth-mass planets is not feasible, with NWO, Super-Earth-type rocky planets are detectable in the habitable zones of solar-analog stars out to distances of at least 5 parsecs.

1.0 Introduction

The majority of extra-solar planet discoveries have been achieved using line-of-sight Doppler detection of stellar reflex motion [Marcy & Butler, 1998]. A smaller percentage of detections has resulted from detection of photometric transits [Mazeh et al., 2000], and a few recent detections have been made by direct imaging of large planets at relatively large distances from their stars [Kalas et al., 2008].

Astrometry has been proposed as an alternative planet detection method. Astrometry at the level of accuracy needed to achieve planet detection is not possible from the ground, but has been proposed for a variety of space missions, e.g., SIM [Shao et al., 2007] and Gaia [Lattanzi et al., 2005]. Direct detection of an Earth-mass planet orbiting a Solar-like star at a distance of 10 pc has been shown to be possible if such missions can reach 1 μas positional accuracy.

Even at reduced accuracies, astrometry can be used to detect the reflex motion induced in a central star by orbiting planets. With a base-line single measurement positional accuracy of 4 μas, the New Worlds Observer (NWO) primary telescope could serve as a potential flagship mission for such astrometric planetary studies.

Doppler and photometric detection are best at detecting large planets in close-in orbits. As a result, the current set of known extra-solar planets is heavily skewed to "hot Jupiters;" i.e., gas giants orbiting at close distances to the central star. However, current planetary evolution theory suggests that these gas giants form much farther away from the central star and migrate in, and in doing so, completely disrupt any terrestrial planets in habitable zones (HZs) [Raymond, S.N., Quinn, T., & Lunine, J.I. 2005]. These methods are therefore not the most conducive to detecting Solar-analog systems. On the other hand, the astrometric method favors detection of targets that are farther out rather than closer in. Quantification of the frequency of such "cold Jupiters" is critical for developing target lists for instruments capable of detecting terrestrial planets as well as advancing our knowledge and understanding of the evolutionary development of stellar systems.

In addition to quantifying the preponderance of habitable solar systems, detection of habitable planets with masses a few times the mass of the Earth may also be possible with NWO astrometric precision capabilities. In the following sections we derive the detection limits for both habitable and gas-giant planets using NWO parameters. We examine these detection limits as a function of the spectral type of the host star and distance to these stars. Finally we summarize the projected detection capabilities of the NWO primary instrument.

2.0 Astrometric Planet Detection with NWO

2.1 Planetary Detection Limit

The parameters and requirements for the astrometric telescope place constraints on the mass of detectable planets and limitations on their orbital properties. In astrometric observations, the presence of the planet is inferred from the motion of the star around the gravitational center or barycenter of the system. The error floor of the instrument determines how accurately this reflex motion can be determined. In general, in order to collect enough data for an accurate determination of the orbital parameters, it is desirable to observe at least half of the orbit (i.e. half of the ellipse). This means for a telescope with a 5 to 10 year mission lifetime, we would expect to obtain good data for planets with orbital periods up to 10 to 20 years. This section derives the relationship between detectable planet mass and distance to the system for an astrometric instrument with a single measurement precision capability of 4μas[1].

The reflex motion induced on a star by an orbiting planet is a function of the orbital parameters of the planet and the mass ratio of the system. Specifically the reflex motion is given by:

$$RM = \frac{m_p a}{M_*} \tag{4}$$

where a is the semi-major axis of the planetary orbit, m_p is the mass of the planet and M_* is the mass of the star. The spectral types of the stars examined in this analysis and their masses are given in Table 1. The semi major axis can be calculated using Kepler's third law and is written:

$$a = \left(\frac{P^2 G\left(M_* + m_p\right)}{4\pi^2} \right)^{\frac{1}{3}}, \tag{5}$$

where P is the period of the orbit and G is the gravitational constant. In this initial analysis a period of 10 and 20 years is used and is derived from an assumed mission lifetime of 5-10 years

The astrometric signal (i.e., the apparent wobble of the star in the sky due to orbital motion about the star-planet center of mass) expected from such a reflex motion is dependent on the distance to the object and is given by:

$$Sig = \frac{RM}{d}. \tag{6}$$

Rewriting equations (4), (5) and (6) above, the relationship between mass of detectable planets and distance to the system can be calculated:

$$d = \left(\frac{m_p}{Sig \times M_*} \right) \left(\frac{P^2 G\left(M_* + m_p\right)}{4\pi^2} \right)^{\frac{1}{3}}. \tag{7}$$

This relationship is used in the following section to estimate the minimum detectable planetary mass as a function of spectral type and distance for the NWO instrument.

---

[1] 4μas is the current, internal NWO estimate for the astrometric single measurement systematic error floor (Noecker et al. 2008).

Table 1: Spectral Types, Absolute Magnitudes and Masses for Main Sequence Stars.

Spectral Type	M(V)	M(I)	$M_*/M_\odot$
F0	2.70	2.23	1.60
F5	3.50	2.86	1.40
G0	4.40	3.59	1.05
G5	5.10	4.21	0.92
K0	5.90	4.84	0.79
K5	7.35	5.73	0.67
M0	8.80	6.61	0.51
M2	9.90	7.21	0.40
M5	12.30	8.83	0.21

Reference: Allen's Astrophysical Quantities

2.2 Detectable Planet Masses and Orbits

Assuming a 5-10 year mission lifetime and a single measurement precision of 4μas, we have calculated the projected detectable planetary mass as a function of distance to the system for each spectral type identified in Table 1. We adopt a three-sigma detection criterion, resulting in a 12μas astrometric signal requirement. In Figures 1 and 2 we plot this relationship for a mission lifetime of 5 and 10 years respectively. In each plot the masses of Earths, super-Earths, Jupiters, and gas-giants are plotted as horizontal, dotted lines. In Figures 3 and 4 we plot the annular distance from the Earth around which Earth and Jupiter-mass planets can be observed for an NWO-class mission. This annulus is shown as a function of spectral type and total mission lifetime.

As can be seen from Figures 1-4, planets with masses similar to Earth can be detected around stars 3 to 5 parsecs away. In particular, late type stars, such as M-stars are the most likely candidates for earth-mass planet detection. For a 5 year mission lifetime, these are the only stars around which can expect to detect such planets astrometrically. However, for a 10 year mission lifetime earth-sized planets can also be detected around K and G stars out to about 5 parsecs. We note that the orbital periods for such planets are large: 10 and 20 years respectively. Such planets are not habitable since the presence of liquid water is doubtful at orbits at such large radial distances from the host star.

Figure 1: Mass of Planets as a function of Distance for a 5 year Mission Lifetime

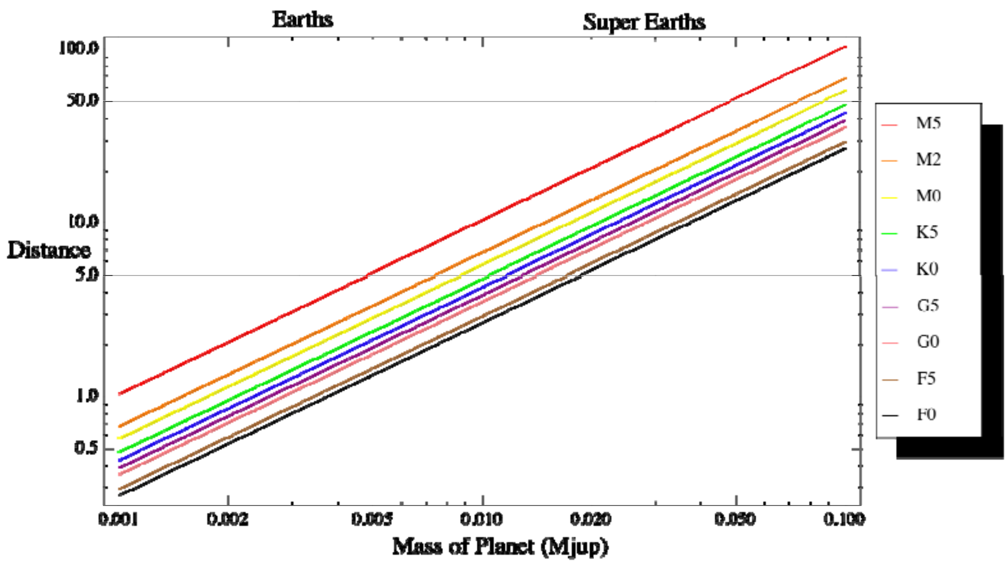

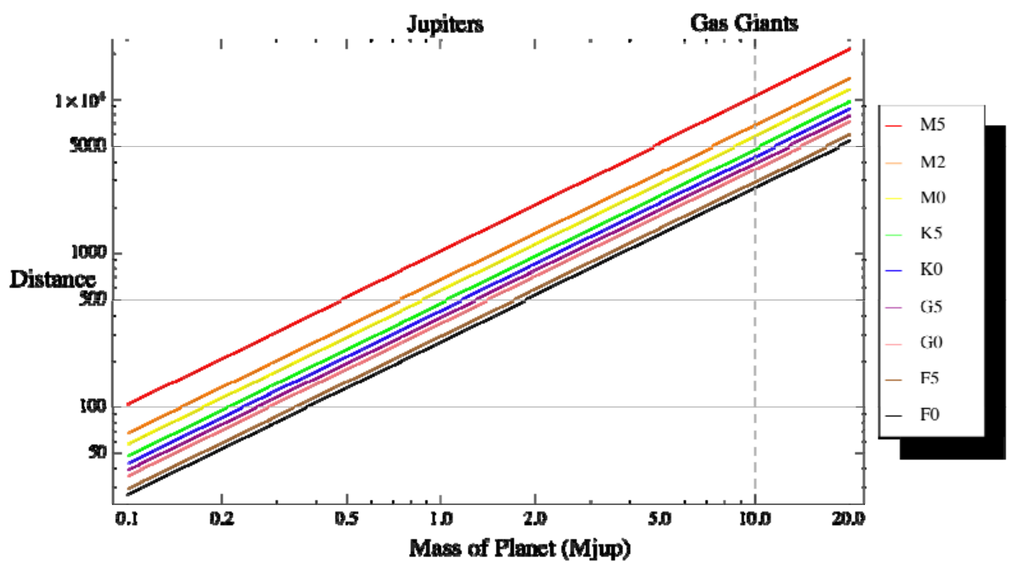

Notes: Figures 1a and 1b show the detectable planet mass as a function of distance (in parsecs) for planets with masses in the range of earth sizes and Jupiter sizes respectively. This calculation assumes a 5-year mission lifetime or a maximum orbital period of 10-years. Note that Earth sized planets are most likely to be detected around late-type stars—especially M stars—out to a distance of about 3 parsecs. However, Earth-mass planets cannot be detected around F stars or those with earlier spectral types.

Figure 2: Mass of Planets as a function of Distance for a 10 year Mission Lifetime

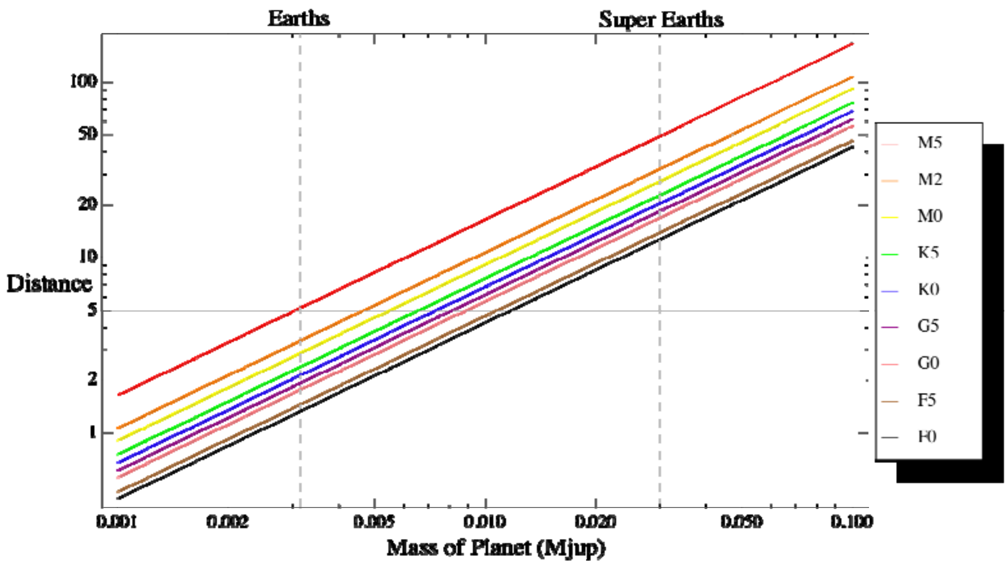

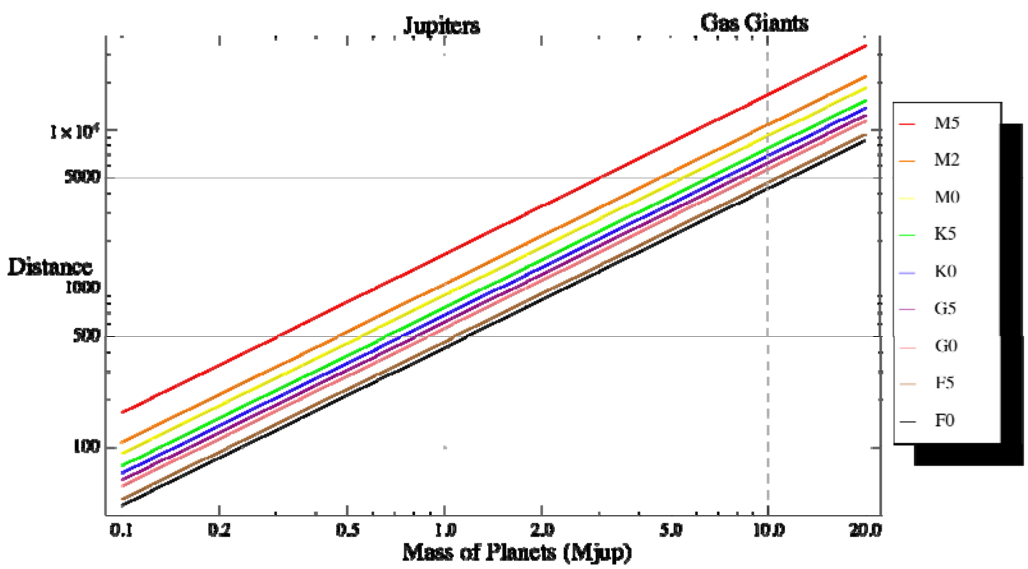

Notes: Figures 2a and 2b show the detectable planet mass as a function of distance (in parsecs) for planets with masses in the range of earth sizes and Jupiter sizes respectively. This calculation assumes a 10-year mission lifetime or a maximum orbital period of 10-years. Here too Earth sized planets are most likely to be detected around late-type stars, however in this case these planets can also be detected around earlier type K stars out to ~2 parsecs.

Figure 3: Distance To Stars with Detectable Earth and Jupiter-sized Planets (5yr)

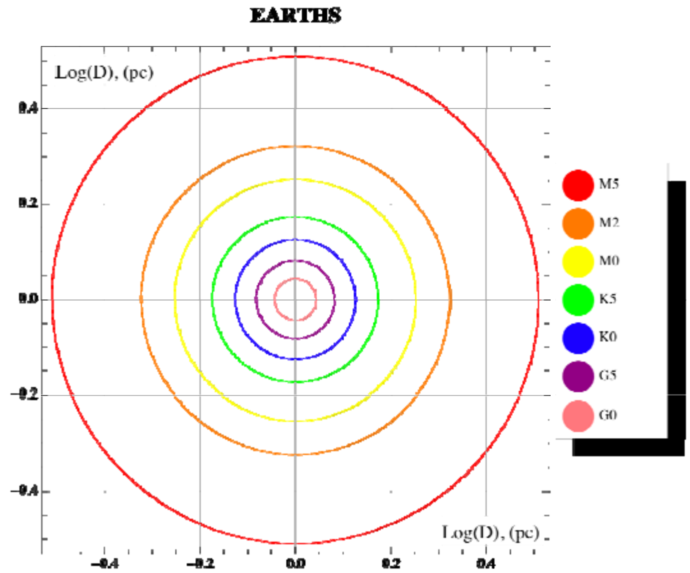

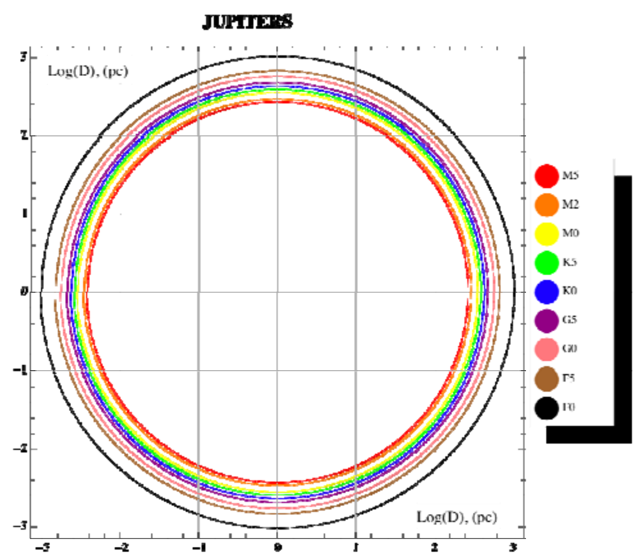

Notes: Figures 3a and 3b describe the annulus out to which stars with Earth- or Jupiter-sized planets can be detected for a 5-year mission lifetime. Earth-mass planets cannot be detected around stars with spectral type F or earlier.

Figure 4: Distance To Stars with Detectable Earth and Jupiter-sized Planets (10yr)

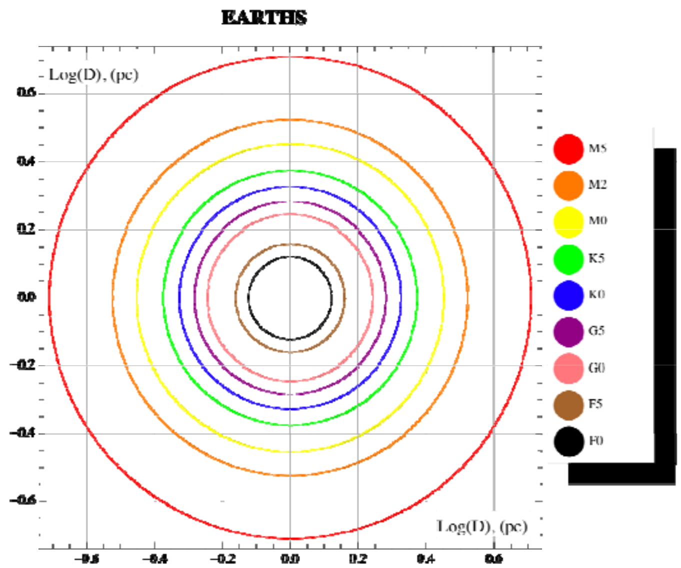

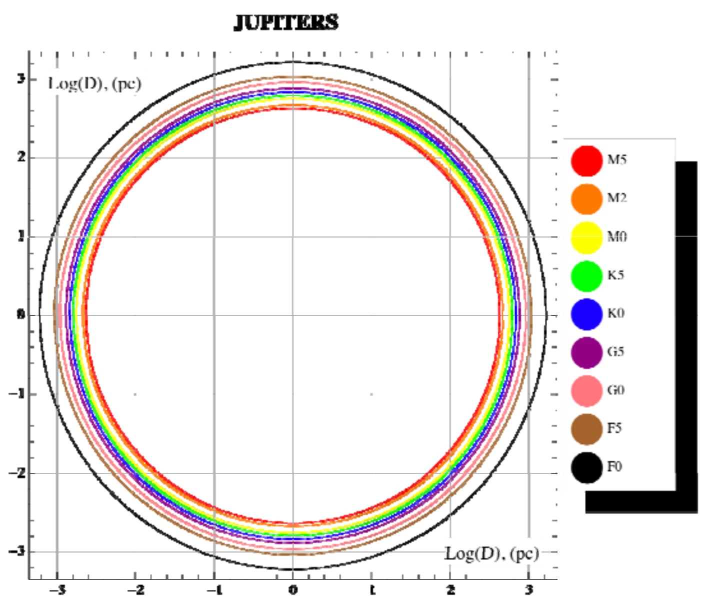

Notes: Figures 4a and 4b describe the annulus out to which stars with Earth- or Jupiter-sized planets can be detected for a 10-year mission lifetime.

Figures 1-4 also show that Jupiter-mass planets and gas-giants are detectable around stars out to over 10 kilo-parsecs. Here too, the orbital periods are quite large. Indeed a 20 year orbit requires a radial distance from the star of at least 8 AU; a distance which classifies these objects as “cold Jupiters.” Such planets are now thought to be signatures of solar-systems most likely to host habitable earth analogs.

2.3 Detecting Habitable Planets

The analysis in §2.1 and §2.2 describes the detection limits of the instrument for planets with masses in the range of Earths to gas giants. However these planetary detection limits are based on mission lifetime, implying large orbital radii that are potentially well outside the habitable zone. The habitable zone here is defined as the range in radii from the star at which a planet must orbit for water to exist in liquid form on the planetary surface. This range in radii is a function of spectral type and luminosity. The central radius of this habitable zone for a star of any spectral type is calculated so that the incident flux on the planet from any star is equal to that on the Earth:

$$\frac{L}{L_{\otimes}} = \frac{4\pi a^2 F}{4\pi a_{\otimes}^2 F} = \left(\frac{a}{a_{\otimes}}\right)^2, \qquad (8)$$

where a_o is the semi-major axis of the Earth’s orbit or 1-AU. The central radius of the habitable zone for a star of any spectral type is:

$$a = \sqrt{\frac{L}{L_{\otimes}}} \qquad (9)$$

Kasting, Whitmire, and Reynolds (1993) estimate that the boundaries for the habitable zone around a star like the Sun are between 0.95 and 1.15-AU. This corresponds to a minimum and maximum radial boundary of 95% and 115% of the central radius for a star of any spectral type. Table 2 below lists the luminosities and the minimum, central and maximum habitable zone distances for the stellar spectral types F0 to M5.

Table 2: Stellar Luminosities and Habitable Zone Range

Spectral Type	log ($L/L_{\odot}$)	HZ Min *a* (AU)	HZ Central *a* (AU)	HZ Max *a* (AU)	Max Period (years)
F0	0.81	2.40	2.53	3.46	5.10
F5	0.54	1.77	1.86	2.55	3.45
G0	-0.04	0.91	0.95	1.31	1.47
G5	-0.30	0.67	0.70	0.96	0.98
K0	-0.60	0.48	0.50	0.69	0.65
K5	-0.90	0.34	0.36	0.49	0.42
M0	-1.35	0.20	0.21	0.29	0.22
M2	-1.70	0.13	0.14	0.19	0.13
M5	-2.37	0.06	0.07	0.09	0.06

Notes: Luminosities were derived from the mass-luminosity data presented in Allen’s Astrophysical Quantities

Formatted: French (France)

In Figure 5 we plot the projected semi-major axis of the planetary orbit as a function of stellar mass for the detection limit of the instrument (Equation 5) and for planets in the habitable zone (Equation 9). In this figure, we see clearly that the HZ requirement constrains the semi-major axis of a target planet, with the result that the astrometric signal is diminished and the planet more difficult to detect. The semi-major axis of the orbit for habitable planets decreases drastically as stellar mass decreases, making habitable planets with late-type stellar hosts very difficult to detect astrometrically. On the other hand, late-type stellar hosts remain excellent candidates for detecting cold Jupiters, and thus identifying candidate solar systems, even if direct detection of planets in the HZ is extremely difficult astrometrically.

Figure 5: Semi-Major Axis as a function of the Mass of the Host Star

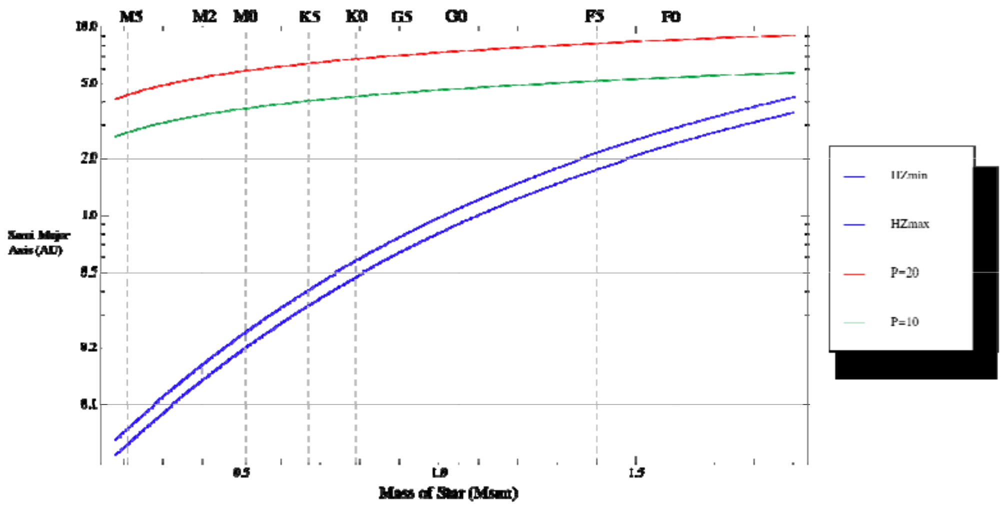

To calculate the detection limit for habitable earth-like planets detectable for an NWO-class mission, equations (4) and (6) above were combined:

$$d = \frac{m_p a}{Sig \times M_*}. \qquad (10)$$

Here the semi-major axis, *a*, is the radius from the star to the planet in the habitable zone. For this detection limit calculation, the semi-major axis was chosen to be the outer (maximum) habitable zone annulus, since this radius provides the maximum astrometric signal.

In Figure 6 we plot the habitable planet mass as a function of distance to the star for stars in the spectral range F0-M5. In this calculation we only examine planets with masses in the Earth to Super-Earth (rocky planets with masses between 1-10 Earth masses) range. We again assume a 3-sigma, 12μas astrometric detection limit.

From this plot, Earth-sized habitable planets will not be detected by NWO with 3-sigma certainty. However, with 4μas single measurement precision, Super-Earths can be detected out to 5 parsecs.

Figure 5: Detectable Habitable Planets

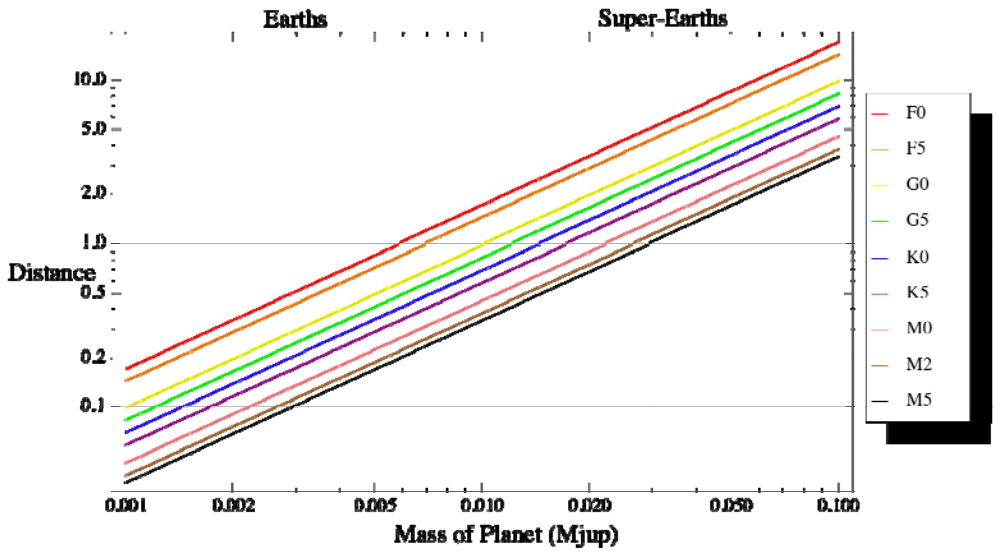

Notes: Figure 5 plots the mass of the habitable planet as a function of distance to the star and stellar spectral types. While detection of habitable Earth-mass planets is unlikely, Super-Earths can be detected out to distances of 5 parsecs.

3.0 Summary

In this paper we have examined the astrometric, planetary detection limits for an NWO-class mission, one with astrometric accuracies as precise as 4μas. We find that Earth-sized planets can be detected out to 5 parsecs for late-type stars, but will have orbits far outside the habitable zone. On the other hand, "cold Jupiters" can be detected out to distances exceeding 1 kilo-parsec and gas-giants out to 10 kilo-parsecs. Such planets are thought to be signatures of habitable solar-systems and NWO-class observations can be used to identify target systems for follow-up with other instruments, including the NWO occultor. Finally we examined the capability of an NWO-class mission to astrometrically detect habitable planets around nearby stars. While astrometric detection of habitable earth analogs is not possible with the base-line positional accuracy of NWO, Super-Earths will be detectable in the habitable zones of solar-analog stars out to distances of at least 5 parsecs.

4.0 References

1. Marcy, G.W., & Butler, R.P. 1998, Brown Dwarfs and Extrasolar Planets, 134, 128
2. Mazeh, T., et al. 2000, ApJL, 532, L55 **Formatted:** French (France)
3. Kalas, P., et al. 2008, Science, 322, 1345
4. Shao, M., Unwin, S.C., Beichman, C., Catanzarite, J., Edberg, S.J., Marr, J.C., IV, & Marcy, G. 2007, Proc. SPIE, 6693
5. Lattanzi, M. G., Casertano, S., Jancart, S., Morbidelli, R., Pourbaix, D., Pannunzio, R., Sozzetti, A., & Spagna, A. 2005, The Three-Dimensional Universe with Gaia, 576, 251
6. Raymond, S.N., Quinn, T., & Lunine, J.I. 2005, Icarus, 177, 256 **Formatted:** French (France)
7. Allen's Astrophysical Quantities, Cox, A., 2000, Athlone Press, London
8. Kasting, Whitmire, and Reynolds, 1993, ICAR, 101,108
9. Noecker, C., 2008, Private Communication.